

Composite solitary waves in three-component scalar field theory: I. The kink variety.

A. Alonso Izquierdo^(a) and J. Mateos Guilarte^(b)

^(a) *Departamento de Matematica Aplicada, Universidad de Salamanca, SPAIN*

^(b) *Departamento de Fisica Fundamental and IUFFyM, Universidad de Salamanca, SPAIN*

Abstract

We study the structure of the manifold of solitary waves in a particular three-component scalar field theoretical model in two-dimensional Minkowski space. These solitary waves involve one, two, three, four, six or seven lumps of energy.

1 Introduction

The search for solitary waves is a mandatory topic in a huge number of branches of non-linear science. The reason for this lies in the fact that the method of linearizing nonlinear differential equations omits phenomena of essential importance in many different physical problems. The non-linear Klein-Gordon system of coupled PDE equations, generalized to n -real scalar fields, reads:

$$\frac{\partial^2 \phi_a}{\partial t^2} - \nabla^2 \phi_a + \frac{\partial V}{\partial \phi_a} = 0 \quad a = 1, 2, \dots, N \quad . \quad (1)$$

Here, $V(\phi_1, \dots, \phi_n)$ is a differentiable potential function of the scalar fields ϕ_a , whereas $\frac{\partial V}{\partial \phi_a}$ are non-linear functions of the fields. It is clear that this system is invariant under Poincare transformations. For this reason we shall use a system of units where the speed of light is set to one: $c = 1$. Also, due to the potential applications of the PDE system (1) in quantum physics we shall implicitly understand $\hbar = 1$, i.e., we shall work in the natural system of units.

We shall focus on physical systems governed by the PDE system (1) in only one spatial dimension. The paradigm with only one real scalar field is the celebrated sine-Gordon equation:

$$\frac{\partial^2 \phi}{\partial t^2} - \frac{\partial^2 \phi}{\partial x^2} + \sin \phi = 0$$

Arising in differential geometry in the theory of negative curvature surfaces, the sine-Gordon equation is ubiquitous in the description of one-dimensional physical phenomena. To mention a few, 1) it is the evolution equation for the amplitude of various slowly varying waves, 2) it describes the propagation of a dislocation in a crystal, 3) it provides a model for elementary particles moving on a line, 4) it rules the propagation of magnetic flux in a long Josephson-junction transmission line, 5) it determines the modulation of a weakly unstable baroclinic wave packet in a two-layer fluid, etcetera, see, e.g., Reference [1].

Point 3) deserves special mention and will be the arena within we shall analyze the generalized non-linear Klein-Gordon PDE system proposed in this paper. The similarities between the properties of solitary waves (or solitons) and elementary particles are clear. The field energy density of a non-linear wave (solitary wave or soliton) is localized in a lump. Moreover, being non-dispersive, solitary waves

(or solitons) propagate without changes in shape. After collisions, solitary waves almost keep their structure, leaving some radiation in the form of dispersive waves as remnants. Solitons, however, only suffer phase shifts under collisions. In soliton-antisoliton scattering, either both solitary waves may be annihilated or, alternatively, they may form a bound (breather) state. Elementary particles share all of these properties. Thus, if an appropriate system of non-linear field equations admits solitary waves (or solitons) as solutions, these non-dispersive waves behave almost as elementary particles.

Nevertheless, the main feature of these solutions, the confinement of the energy density, has straightforward implementation in many areas. In Condensed Matter, these solutions describe interfaces in magnetic materials [2] and in ferroelectric crystals [3]. They have also been used to understand some bizarre properties of the poly(oxyethylene) [4], widely studied owing to its biotechnical and biomedical applications [5]. Among the impressive features of this polymer, we can mention the ability to entrap metallic ions in aqueous solution and its solubility in water to almost any extent. On the other hand, in Cosmology solitary waves are interpreted as domain walls which seeded the formation of structures in the early universe [6]. They are also of direct interest in high energy physics, for instance, describing gravity in warped spacetimes involving D extra spatial dimensions [7], or the coupling of scalar matter fields with dilaton gravity [8], which seems to be related to the formation and evaporation of black holes [9]. Furthermore, when these defects appear as BPS states in both extended supersymmetric gauge theories [10] and string/M theory [11] they play a crucial rôle in the understanding of dualities between the different regimes of the system. In this framework, they behave as extended states in $\mathcal{N} = 1$ SUSY gluodynamics and the Wess-Zumino model [12]. The structure of the solitary waves that we are going to unveil in this paper is richer than the usual kink structure found in simpler models. Thus, our topological defects could describe more subtle effects in each of all these scenarios.

In general, the above mentioned systems involve a high number of fields. In order to investigate the presence of solitary waves or topological defects, the usual procedure is to obtain an effective scalar field theory, carrying out severe restrictions on the original theory. In most cases one is compelled to pursue an effective theory that corresponds to a single scalar field model, where the existence of topological defects can be checked easily. In general, however, the effective theory depends on several scalar fields, and the truncation can involve a important loss of information about the presence of solitary waves or topological defects. Therefore, it is desirable to investigate the general properties of solitary waves in a multi-scalar field theory. This is an important qualitative step as reported by Rajaraman [13]: *This already brings us to the stage where no general methods are available for obtaining all localized static solutions, given the field equations. However, some solutions, but by no means all, can be obtained for a class of such Lagrangians using a little trial and error.*

Some work on two-component scalar field theory models equipped with a Minkowskian space-time has been accomplished, see for instance References [14, 15, 16, 17, 18, 19, 20, 21]. In some of these models, two-parametric families of solitary waves or kinks are identified. Generally, each member of these families is a composite solitary wave, which involves several lumps, i.e, the energy density is localized at several points. The parameters identifying each solution correspond to a translational parameter, x_0 , which determines the center of the kink, and an “orbit” parameter b , which specifies the separation between the lumps. Study of Manton’s adiabatic motion of solitary waves [22] is very simple in this case because the geometric metric of the moduli (parameter) space that governs the dynamics does not depend on the translational parameter x_0 ; thus, it is always possible to apply a transformation that leads to an Euclidean metric. On the other hand, there are only a few works that have addressed research into solitary waves in three-component scalar field theory models, see [23, 24, 25, 26]. In this richer case there are three-parametric families of kinks, and the adiabatic evolution of three-body lumps is associated with metrics with curvature. The low-energy dynamics of, in this case, three-body solitary waves is therefore much more intricate.

In a slightly different physical context, where the solitary waves are understood as domain walls

(2-branes) in (3+1) dimensions models with three scalar fields have been discussed in Reference [27]. Considering topological defects (0-branes) in more spatial dimensions (p-branes) allows for complex structures having defects nested inside defects. It is plausible that the composite solitary waves to be discussed in this paper will give rise to even richer structures of nested defects inside defects if considered in more dimensions. An interesting work is also available on networks of topological defects in a model with two complex scalar fields, see [28]. The potential energy density is a polynomial in the fields of arbitrary order chosen in such a way that the model enjoys a $U(1) \times \mathbb{Z}_n$ symmetry, networks of domain walls arising in the surface of Q -balls. In other direction, defects inside defects in models with two scalar fields have been considered before, see [29] and [30]. Very recently, networks of topological defects arising in a model with $9n$ scalar fields in nine spatial dimensions have been studied in [31] and the evolution of these (or similar) structures has been analyzed in [32].

In this paper, we shall address a three-component scalar field model that generalizes the two-component model discussed in Reference [14] to three fields. The organization of the paper is as follows: in Section 2 we introduce the model and describe the spontaneous symmetry breaking pattern as well as the spectrum of dispersive waves. In Section 3 we describe the variety of solitary (non-dispersive) waves that arises in this system. We classify these solutions according to the number of lumps they are made of. There are three basic solitary waves with the energy density confined in one finite region. The rest of the solutions are composite and display several lumps –the energy density is localized at various points–.

2 Deformation of the $\lambda(\vec{\phi} \cdot \vec{\phi})_2^3$ -model

We shall deal with a three-component scalar field theory model defined in a (1+1) Minkowskian space-time. The dynamics is governed by the action functional:

$$S = \int d^2x \left[\frac{1}{2} \partial_\mu \phi^a \partial^\nu \phi^a - V(\phi_1, \phi_2, \phi_3) \right] \quad (2)$$

and the potential term is the following sixth-degree polynomial in the fields:

$$V(\vec{\phi}) = (\phi_1^2 + \phi_2^2 + \phi_3^2)(\phi_1^2 + \phi_2^2 + \phi_3^2 - 1)^2 + 2(\sigma_2^2 \phi_2^2 + \sigma_3^2 \phi_3^2)(\phi_1^2 + \phi_2^2 + \phi_3^2 - 1) + \sigma_2^4 \phi_2^2 + \sigma_3^4 \phi_3^2 \quad . \quad (3)$$

σ_2 and σ_3 are the non-dimensional coupling constants of the system, chosen, without loss of generality, such that $\sigma_2 < \sigma_3$. ϕ^a , $a = 1, 2, 3$, are dimensionless scalar fields,

$$\vec{\phi}(x_0, x_1) = (\phi_1(x_0, x_1), \phi_2(x_0, x_1), \phi_3(x_0, x_1)) : \mathbb{R}^{1,1} \rightarrow \mathbb{R}^3 \quad .$$

Our convention for the metric tensor components in Minkowski space $\mathbb{R}^{1,1}$ is: $g_{00} = -g_{11} = 1$ and $g_{12} = g_{21} = 0$.

This model is a (σ_2, σ_3) deformation of the same system with $SO(3)$ -invariant potential energy density:

$$V_S(\vec{\phi}) = (\phi_1^2 + \phi_2^2 + \phi_3^2)(\phi_1^2 + \phi_2^2 + \phi_3^2 - 1)^2 \quad (4)$$

Besides the Poincare transformations acting on $\mathbb{R}^{1,1}$, the non-deformed model $-\sigma_2 = \sigma_2 = 0$ - is invariant under $O(3)$ rotations in internal space \mathbb{R}^3 . The specific form of V_S , however, shows spontaneous symmetry breaking of the internal symmetry to a $SO(2)$ subgroup so that two Goldstone bosons are unavoidable if the asymmetric vacuum -any point at a distance 1 from the origin in \mathbb{R}^3 - is chosen to perform the quantization of the system; the set of zeroes of V_S is the the union of a discrete point, the origin, and a continuous manifold, the 2-sphere of radius 1 in \mathbb{R}^3 . Coleman proved in [33] that there are no Goldstone bosons on the line in a sensible physical system. The infrared asymptotic behavior of the quantum system would require modification of the potential V_S in such a way that the zeroes of the potential become a

discrete set and massless particles are forbidden. Our deformation complies with this requirement and could be understood as being generated by infrared quantum fluctuations. The added terms in the potential (3) explicitly break the $O(3)$ symmetry to the discrete subgroup $\mathbb{G} = \mathbb{Z}_2 \times \mathbb{Z}_2 \times \mathbb{Z}_2$, generated by the reflections $\phi_1 \rightarrow -\phi_1$, $\phi_2 \rightarrow -\phi_2$ and $\phi_3 \rightarrow -\phi_3$ in internal space. We also stress that the present system is a generalization of the two-component scalar field theory model discussed in Reference [14], where the dimension of the internal space, the number of scalar fields, is increased by one unit.

The field equations form the system of coupled second-order partial differential equations:

$$\begin{aligned} \frac{\partial^2 \phi_1}{\partial t^2} - \frac{\partial^2 \phi_1}{\partial x^2} &= 2\phi_1 [3(\phi_1^2 + \phi_2^2 + \phi_3^2)^2 + 1 - 4\phi_1^2 - 2(2 - \sigma_2^2)\phi_2^2 - 2(2 - \sigma_3^2)\phi_3^2] \\ \frac{\partial^2 \phi_2}{\partial t^2} - \frac{\partial^2 \phi_2}{\partial x^2} &= 2\phi_2 [3(\phi_1^2 + \phi_2^2 + \phi_3^2)^2 - 2(2 - \sigma_2^2)\phi_1^2 - 4\bar{\sigma}_2^2\phi_2^2 - 2(\bar{\sigma}_2^2 + \bar{\sigma}_3^2)\phi_3^2 + \bar{\sigma}_2^4] \\ \frac{\partial^2 \phi_3}{\partial t^2} - \frac{\partial^2 \phi_3}{\partial x^2} &= 2\phi_3 [3(\phi_1^2 + \phi_2^2 + \phi_3^2)^2 - 2(2 - \sigma_3^2)\phi_1^2 - 2(\bar{\sigma}_2^2 + \bar{\sigma}_3^2)\phi_2^2 - 4\bar{\sigma}_3^2\phi_3^2 + \bar{\sigma}_3^4] \end{aligned} \quad (5)$$

For the sake of simplicity, henceforth we use the notation: $x_0 = t$, $x_1 = x$, $\bar{\sigma}_2 = \sqrt{1 - \sigma_2^2}$, $\bar{\sigma}_3 = \sqrt{1 - \sigma_3^2}$, $\sigma_{32}^2 = \sigma_3^2 - \sigma_2^2$.

2.1 Structure of the configuration space

A ‘‘point’’ in the configuration space of the system is a configuration of the field of finite energy; i.e., a picture of the field at a fixed time such that the energy E , the integral over the line of the energy density,

$$E[\vec{\phi}] = \int_{-\infty}^{\infty} dx \mathcal{E}[\vec{\phi}] \quad , \quad \mathcal{E}[\vec{\phi}] = \frac{1}{2} \left(\frac{d\phi_1}{dx} \right)^2 + \frac{1}{2} \left(\frac{d\phi_2}{dx} \right)^2 + \frac{1}{2} \left(\frac{d\phi_3}{dx} \right)^2 + V(\phi_1, \phi_2, \phi_3) \quad , \quad (6)$$

is finite. Thus, the configuration space is the set of continuous maps from \mathbb{R} to \mathbb{R}^3 of finite energy:

$$\mathcal{C} = \left\{ \vec{\phi}(x) \in \text{Maps}(\mathbb{R}, \mathbb{R}^3) / E < \infty \right\} \quad .$$

In order to belong to \mathcal{C} , each configuration complies with the asymptotic conditions

$$\lim_{x \rightarrow \pm\infty} \vec{\phi} \in \mathcal{M} \quad \lim_{x \rightarrow \pm\infty} \frac{d\vec{\phi}}{dx} = 0 \quad (7)$$

where \mathcal{M} is the set of zeroes (minima) of the potential term $V(\vec{\phi})$. In our model, \mathcal{M} consists of seven elements, see Figure 1:

$$\mathcal{M} = \left\{ \bar{\phi}^O \equiv (0, 0, 0); \quad \bar{\phi}^{D^\pm} \equiv (\pm 1, 0, 0); \quad \bar{\phi}^{B^\pm} \equiv (0, 0, \pm \bar{\sigma}_3); \quad \bar{\phi}^{C^\pm} \equiv (0, \pm \bar{\sigma}_2, 0) \right\} \quad (8)$$

Note that all the zeroes except the origin lie in the ellipsoid $\mathbb{E} \equiv \phi_1^2 + \frac{\phi_2^2}{\sigma_2^2} + \frac{\phi_3^2}{\sigma_3^2} = 1$. The intersections of the ellipsoid \mathbb{E} and the $\phi_1 = 0$, $\phi_2 = 0$, $\phi_3 = 0$ -planes are respectively the ellipses $e_1 \equiv \frac{\phi_2^2}{\sigma_2^2} + \frac{\phi_3^2}{\sigma_3^2} = 1$, $e_2 \equiv \phi_1^2 + \frac{\phi_3^2}{\sigma_3^2} = 1$ and $e_3 \equiv \phi_1^2 + \frac{\phi_2^2}{\sigma_2^2} = 1$ of eccentricities $\varepsilon(e_1) = \frac{\sigma_{32}^2}{\sigma_2^2}$, $\varepsilon(e_2) = \sigma_3^2$ and $\varepsilon(e_3) = \sigma_2^2$. The minima B_\pm are on the ϕ_3 -axis at the intersection between e_1 and e_2 ; C_\pm lies on the ϕ_2 -axis at $e_1 \cap e_3$, and D_\pm on the ϕ_1 -axis at $e_2 \cap e_3$.

The configuration space \mathcal{C} is the union of 49 topologically disconnected sectors:

$$\mathcal{C} = \cup_{I,J} \mathcal{C}^{IJ}$$

where $I, J = \{O, D, C, B\}$ and \mathcal{C}^{IJ} stands for the set of configurations that connect the points $\bar{\phi}^I$ with $\bar{\phi}^J$. Because temporal evolution is a homotopy transformation, the asymptotic conditions (7) do not change with t and the sectors are completely disconnected. Physically, this means that a configuration in a sector cannot evolve into configurations in other different sectors; it would cost infinite energy.

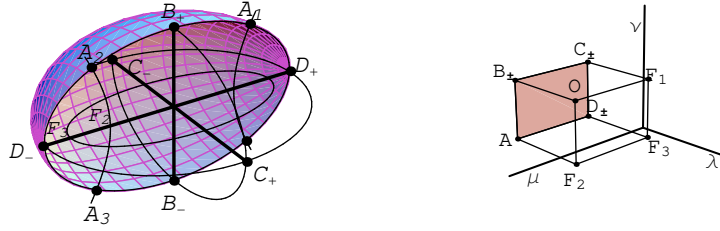


Figure 1: *Points belonging to \mathcal{M} , umbilical points, focal points, and characteristic curves of the model drawn on and inside the ellipsoid \mathbb{E} : (left) Cartesian coordinates. (right) Elliptic coordinates.*

2.2 Plane waves and spontaneous symmetry breakdown

The zeroes of the potential energy density (8) are also homogeneous static solutions of the field equations (5) with zero energy; in fact, they are absolute minima of the energy in the topological sectors \mathcal{C}^{II} . A spontaneous symmetry breaking arises because of the degeneracy of the set \mathcal{M} . Whereas the point $\bar{\phi}^O$ located in the origin preserves the discrete symmetry $\mathbb{Z}_2 \times \mathbb{Z}_2 \times \mathbb{Z}_2$ of the Lagrangian, the choice of $\bar{\phi}^{D^\pm}$ breaks the symmetry generated by the reflection $\phi_1 \rightarrow -\phi_1$, which connects the two points, $\bar{\phi}^{D^+}$ and $\bar{\phi}^{D^-}$, to the little group $\{e\} \times \mathbb{Z}_2 \times \mathbb{Z}_2$. Similar considerations work for the pair of points $\bar{\phi}^{C^\pm}$ and $\bar{\phi}^{B^\pm}$ with respect to the transformations $\phi_2 \rightarrow -\phi_2$ and $\phi_3 \rightarrow -\phi_3$. The moduli space of vacua comprises four \mathbb{G} -orbits

$$\bar{\mathcal{M}} = \frac{\mathcal{M}}{\mathbb{G}} = \{ \bar{\phi}^O ; \bar{\phi}^D ; \bar{\phi}^B ; \bar{\phi}^C \}$$

where we write $\bar{\phi}^D = \{ \bar{\phi}^{D^+}, \bar{\phi}^{D^-} \}$, $\bar{\phi}^C = \{ \bar{\phi}^{C^+}, \bar{\phi}^{C^-} \}$ and $\bar{\phi}^B = \{ \bar{\phi}^{B^+}, \bar{\phi}^{B^-} \}$.

Small fluctuations around the homogenous static solutions $\bar{\phi}$, $\psi(t, x) = \bar{\phi} + \delta\psi(t, x)$ are still solutions of (5) if the linear PDE system

$$\sum_{b=1}^3 (\square \delta_{ab} + M_{ab}^2(\bar{\phi})) \delta\psi_b(t, x) = 0_a, \quad M_{ab}^2 = \frac{\partial^2 V}{\partial \phi_a \partial \phi_b}(\bar{\phi}) \quad (9)$$

is satisfied. The solution of (9) via the separation of variables $\delta\psi_a(t, x) = \text{Re}(e^{i\omega t}) f_a^\omega(x)$ leads to the spectral problem for the second-order fluctuation –or Hessian– operator:

$$\sum_{b=1}^3 \mathcal{H}_{ab}(\bar{\phi}) f_b^\omega(x) = \sum_{b=1}^3 \left(-\frac{d^2}{dx^2} \delta_{ab} + M_{ab}^2(\bar{\phi}) \right) f_b^\omega(x) = \omega^2 f_a^\omega(x) \quad (10)$$

$\mathcal{H}(\bar{\phi})$ is a diagonal matrix differential operator for the four points of $\bar{\mathcal{M}}$ with a positive definite spectrum; each constant solution belonging to \mathcal{M} is stable. Thus, there are four types of dispersive wave-packet solutions, each one with three branches

$$f_1^\omega(x) = \sin kx, f_2^\omega = f_3^\omega = 0 \quad ; \quad f_1^\omega = 0, f_2^\omega(x) = \sin qx, f_3^\omega = 0 \quad ; \quad f_1^\omega = f_2^\omega = 0, f_3^\omega(x) = \sin px \quad ,$$

living in one of these sectors. The building blocks are these plane waves and the dispersion laws of the corresponding wave packets are respectively determined by the diagonal matrices:

$$M^2(\bar{\phi}^O) = \begin{pmatrix} 2 & 0 & 0 \\ 0 & 2\bar{\sigma}_2^2 & 0 \\ 0 & 0 & 2\bar{\sigma}_3^2 \end{pmatrix} \quad M^2(\bar{\phi}^D) = \begin{pmatrix} 8 & 0 & 0 \\ 0 & 2\bar{\sigma}_2^4 & 0 \\ 0 & 0 & 2\bar{\sigma}_3^4 \end{pmatrix}$$

$$M^2(\bar{\phi}^C) = \begin{pmatrix} 2\bar{\sigma}_3^4 & 0 & 0 \\ 0 & 8\bar{\sigma}_2^4 & 0 \\ 0 & 0 & 2\bar{\sigma}_{32}^4 \end{pmatrix} \quad M^2(\bar{\phi}^B) = \begin{pmatrix} 2\bar{\sigma}_2^4 & 0 & 0 \\ 0 & 2\bar{\sigma}_{32}^4 & 0 \\ 0 & 0 & 8\bar{\sigma}_3^4 \end{pmatrix}$$

The three branches for each type are:

$\bar{\phi}^D$	$\bar{\phi}^C$	$\bar{\phi}^B$	$\bar{\phi}^O$
$\omega^2(k) = k^2 + 8$	$\omega^2(k) = k^2 + 2\sigma_3^4$	$\omega^2(k) = k^2 + 2\sigma_2^4$	$\omega^2(k) = k^2 + 2$
$\omega^2(q) = q^2 + 2\sigma_2^4$	$\omega^2(q) = q^2 + 8\bar{\sigma}_2^4$	$\omega^2(q) = q^2 + 2\sigma_{32}^4$	$\omega^2(q) = q^2 + 2\bar{\sigma}_2^2$
$\omega^2(p) = p^2 + 2\sigma_3^4$	$\omega^2(p) = p^2 + 2\sigma_{32}^4$	$\omega^2(p) = p^2 + 8\bar{\sigma}_3^4$	$\omega^2(p) = p^2 + 2\bar{\sigma}_3^2$

2.3 Solitary waves from integrable dynamical systems

According to Rajaraman [13] “A solitary wave is a localized non-singular solution of any non-linear field equation whose energy density, as well as being localized, has space-time dependence of the form: $\varepsilon(t, x) = \varepsilon(x - vt)$, where v is some velocity vector”. Because we are dealing with a Lorentz invariant system, solutions with a temporal dependence like this are obtained from static solutions by means of a Lorentz velocity transformation: $L(v)\phi(x) = \phi^L(t, x) = \phi\left(\frac{x-vt}{\sqrt{1-v^2}}\right)$.

Thus, the search for solitary waves is tantamount to looking for localized solutions in the $\mathcal{C}^{IJ}, I \neq J$ sector of the ODE system :

$$\frac{d^2\phi_a}{dx^2} = \frac{\partial V}{\partial\phi_a} \quad a = 1, 2, 3 \quad . \quad (11)$$

Understanding the scalar field $\vec{\phi}$ as the *particle position vector*; x as the *particle time* and $U = -V$ as the *particle potential*, this is no more Newton equations describing the motion of a particle in three dimensions in the field of the potential U . Moreover, the energy functional and the energy density (6) of the field theory turns respectively into the action and the Lagrangian of the mechanical system. The Legendre transformation provides the Hamiltonian of the analogous mechanical system:

$$H = \sum_{a=1}^3 p_a \frac{d\phi_a}{dx} - \mathcal{E}[\vec{\phi}, \frac{d\vec{\phi}}{dx}] = \frac{1}{2} \sum_{a=1}^3 p_a(x) \cdot p_a(x) - V(\vec{\phi}(x)) \quad , \quad p_a = \frac{\partial \mathcal{E}}{\partial \phi^a / \partial x} \quad . \quad (12)$$

The Hamiltonian (12) corresponds to a Stäckel separable system. To prove this, we introduce three-dimensional Jacobi elliptic coordinates (λ, μ, ν) in the internal space (ϕ_1, ϕ_2, ϕ_3) , see [23]. In terms of elliptic coordinates, the fields are:

$$\phi_1^2 = \frac{(1-\lambda)(1-\mu)(1-\nu)}{(1-\bar{\sigma}_3^2)(1-\bar{\sigma}_2^2)}; \quad \phi_2^2 = \frac{(\bar{\sigma}_2^2-\lambda)(\bar{\sigma}_2^2-\mu)(\bar{\sigma}_2^2-\nu)}{(\bar{\sigma}_2^2-\bar{\sigma}_3^2)(\bar{\sigma}_2^2-1)}; \quad \phi_3^2 = \frac{(\bar{\sigma}_3^2-\lambda)(\bar{\sigma}_3^2-\mu)(\bar{\sigma}_3^2-\nu)}{(\bar{\sigma}_3^2-\bar{\sigma}_2^2)(\bar{\sigma}_3^2-1)} \quad . \quad (13)$$

The new variables take values in the infinite cuboid

$$-\infty \leq \lambda \leq \bar{\sigma}_3^2 \leq \mu \leq \bar{\sigma}_2^2 \leq \nu < 1$$

which is mapped by the coordinate transformation (13) to a Cartesian octant in \mathbb{R}^3 . Therefore eight points in \mathbb{R}^3 become only one in the cuboid and mapping back solutions in elliptic coordinates to the original Cartesian ones requires a lot of care to reassemble the solution in the total internal space from one octant by imposing continuity of the trajectories and their derivatives. Apparent rebounds on the faces of $P(0)$, see Figure 1, are really continuous in the closed domain in \mathbb{R}^3 bounded by the ellipsoid \mathbb{E} .

In Figure 1 we have plotted the finite elliptic cuboid, denoted by $P(0)$, where (an octant of) the interior of the ellipsoid \mathbb{E} is mapped. The ellipsoid itself is mapped to the $\lambda = 0$ face of $P(0)$, $\mathbb{E} \equiv \lambda = 0$. In elliptic coordinates, the following information is interesting:

- Homogeneous solutions

$$\begin{aligned} \bar{\phi}^O &\equiv (\lambda = \bar{\sigma}_3^2, \mu = \bar{\sigma}_2^2, \nu = 1) & , & \quad \bar{\phi}^D \equiv (\lambda = 0, \mu = \bar{\sigma}_2^2, \nu = \bar{\sigma}_3^2) \\ \bar{\phi}^B &\equiv (\lambda = 0, \mu = \bar{\sigma}_3^2, \nu = 1) & , & \quad \bar{\phi}^C \equiv (\lambda = 0, \mu = \bar{\sigma}_3^2, \nu = 1) \end{aligned}$$

- Ellipses where the homogeneous solutions live:

$$e_1 \equiv \lambda = 0, \nu = 1 \quad ; \quad e_2 \equiv \begin{cases} \lambda = 0 & , \quad \mu = \bar{\sigma}_2^2 \\ \lambda = 0 & , \quad \nu = \bar{\sigma}_2^2 \end{cases} \quad ; \quad e_3 \equiv \lambda = 0, \mu = \bar{\sigma}_3^2$$

- Other special points: F_1, F_2, F_3 (foci of e_1, e_2 and e_3 respectively) and the umbilicus points A of the ellipsoid \mathbb{E} are settled on the vertices of the parallelepiped $P(0)$ in elliptic space:

$$\begin{aligned} F_1 &\equiv (\lambda = \bar{\sigma}_3^2, \mu = \bar{\sigma}_3^2, \nu = 1) & , & & F_2 &\equiv (\lambda = \bar{\sigma}_3^2, \mu = \bar{\sigma}_2^2, \nu = \bar{\sigma}_2^2) \\ F_3 &\equiv (\lambda = \bar{\sigma}_3^2, \mu = \bar{\sigma}_3^2, \nu = \bar{\sigma}_2^2) & , & & A &\equiv (\lambda = 0, \mu = \bar{\sigma}_2^2, \nu = \bar{\sigma}_2^2) \end{aligned}$$

- Special curves such as the ellipse $e_4 \equiv \frac{\phi_1^2}{\sigma_2^2} + \frac{\phi_2^2}{\sigma_{32}^2} = 1$ corresponding to the edge F_1F_3 in $P(0)$ and the hyperbola $h \equiv \frac{\phi_1^2}{\sigma_2^2} - \frac{\phi_2^2}{\sigma_{32}^2} = 1$, the edge F_2A .

$$e_4 \equiv \lambda = \bar{\sigma}_3^2, \nu = \bar{\sigma}_2^2 \quad , \quad h \equiv \mu = \bar{\sigma}_2^2, \nu = \bar{\sigma}_2^2 \quad .$$

We shall see that these curves are focal lines of finite action trajectories in the analogous mechanical system.

In elliptic coordinates, the Hamiltonian (12) of the analogous mechanical system becomes:

$$H = \frac{H_\lambda}{(\lambda - \mu)(\lambda - \nu)} + \frac{H_\mu}{(\mu - \lambda)(\mu - \nu)} + \frac{H_\nu}{(\nu - \lambda)(\nu - \mu)} \quad . \quad (14)$$

Here,

$$\begin{aligned} H_\lambda &= 2P_3(\lambda)p_\lambda^2 + P_4(\lambda); & H_\mu &= 2P_3(\mu)p_\mu^2 + P_4(\mu); & H_\nu &= 2P_3(\nu)p_\nu^2 + P_4(\nu) \\ P_3(x) &= (1 - x)(\bar{\sigma}_2^2 - x)(\bar{\sigma}_3^2 - x) & P_4(x) &= x^2(x - 1)(x - \bar{\sigma}_2^2)(x - \bar{\sigma}_3^2) \end{aligned}$$

Expression (14) is of the Stäckel form. Thus, the analogous mechanical system is Hamilton-Jacobi separable. We will take advantage of this fact in the following Sections in order to identify the variety of solitary waves in the model as the finite action trajectories of the analogous mechanical system.

3 The variety of solitary waves

In this Section we describe the variety of solitary waves in successive stages. The analogous mechanical system encompasses a vast manifold of finite action trajectories in one-to-one correspondence with the solitary waves of the field theoretical model. One-body solitary waves, made of only one lump, can be found by means of Rajaraman's trial orbit method, without the need to use elliptic coordinates. On plugging some specific trial curves into the equations (11), simple solitary waves that we will refer to as basic lumps arise. The trial orbits correspond to some edges of the parallelepiped $P(0)$ shown in Figure 1(b). Later, solutions which comprise several of the basic lumps will be found by restricting the movement to the faces of the parallelepiped $P(0)$ to find solitary waves akin to those discovered in Reference [14]. As a last step, we shall solve the equations (11) in the general case by applying the Hamilton-Jacobi theory with no restrictions.

The system of ODE (11) is invariant under translations $x \rightarrow x - x_0$ and reflections $x \rightarrow -x$ in the spatial parameter x . The first symmetry allows us to localize the center of the solitary wave or kink at an arbitrary point x_0 , whereas the second symmetry connects a kink with its antikink. Henceforth, we shorthand these transformations on x as \bar{x} , i.e., $\bar{x} = (-1)^\delta(x - x_0)$ with $x_0 \in \mathbb{R}$ and $\delta = 0, 1$.

3.1 Solitary waves: basic types

1. K_1^{OB} : The solutions of (11) in the sector C^{OB} , located in the ϕ_3 -axis in internal space, are four-fold, see Figure 2(c):

$$\bar{\phi}_1(x) = 0; \quad \bar{\phi}_2(x) = 0; \quad \bar{\phi}_3(x) = \frac{(-1)^\alpha \bar{\sigma}_3}{\sqrt{1 + e^{2\sqrt{2}\bar{\sigma}_3^2 x}}} \quad (15)$$

Here, $\alpha = 0, 1$ distinguishes between solutions with $\phi_3 > 0$ and $\phi_3 < 0$. We refer to these solutions as K_1^{OB} . Some remarks about this notation: the superscripts specify the elements of $\bar{\mathcal{M}}$ that are connected by the solution and/or the topological sector C^{OB} , where the solitary wave lives. The subscript shows the number of basic particles, lumps or bodies of which a particular solitary wave is made. In Figure 2(a) a $\alpha = \delta = 0$ K_1^{OB} solitary wave of kink shape is depicted; this K_1^{OB+} kink connects the points B_+ and O in $\bar{\mathcal{M}}$ and lives in the C^{OB+} topological sector of the configuration space. In Figure 2(b) its energy density is plotted as a function of x ; because it is localized at a single point we understand these one-body solutions as basic (non-composite) particles. A Lorentz transformation applied to (15) will show this lump of energy to be a solitary (traveling) wave. Integration on the real line provides us with the total energy, which for these solutions is $E(K_1^{OB}) = \frac{\bar{\sigma}_3^4}{2\sqrt{2}}$ and this depends only on the coupling constant σ_3 .

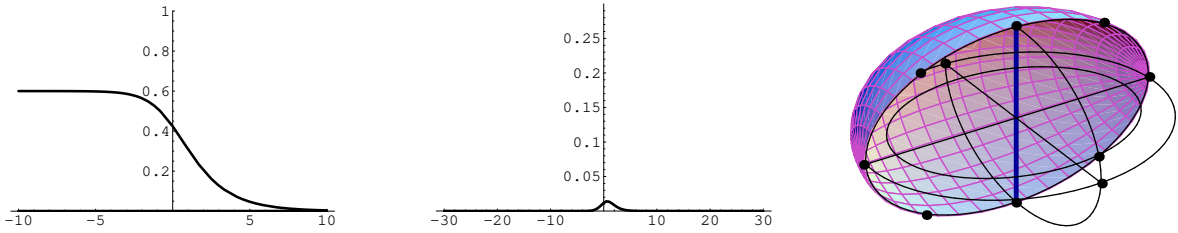


Figure 2: Kink form factor (a), energy density (b) and orbits (c) for K_1^{OB} kinks.

We shall adopt the policy of showing all the energy density plots with the same vertical range in order to compare the size of the lumps associated with different solitary waves.

2. K_1^{CD} : Plugging the trial elliptic orbit $e_3 \equiv \phi_1^2 + \frac{\phi_2^2}{\sigma_2^2} = 1$ into the equations (11) we find the eight solutions

$$\bar{\phi}_1(x) = \frac{(-1)^\alpha}{\sqrt{1 + e^{2\sqrt{2}\sigma_2^2 x}}}; \quad \bar{\phi}_2(x) = \frac{(-1)^\beta \bar{\sigma}_2}{\sqrt{1 + e^{-2\sqrt{2}\sigma_2^2 x}}}; \quad \bar{\phi}_3(x) = 0 \quad (16)$$

with $\alpha, \beta, \delta = 0, 1$. These trajectories are embedded in the $\phi_3 = 0$ plane and live in one of the eight C^{CD} topological sectors, see Figure 3(c). Note that both non-null components, ϕ_1 and ϕ_2 , have kink shape.

The value of δ determines whether the solution is a kink or antikink. The values of α and β , however, characterize the quarter-ellipse in the intersection of the ellipsoid \mathbb{E} with the $\phi_3 = 0$ plane, where a particular solution is located; therefore, α and β also choose the points that are asymptotically connected by these kinks. In Figure 3(a) a particular kink K_1^{CD} with $\alpha = \beta = \delta = 0$ is shown that connects the C_+ and D_+ points. The energy of these kinks is $E(K_1^{CD}) = \frac{\sigma_2^2(2 - \sigma_2^2)}{2\sqrt{2}}$, a function of the coupling constant σ_2 only. Again, the energy density is localized at one point, and they are basic particles in our model, see Figure 3(b).

3. K_1^{BC} : We shall also try the elliptic orbit $e_1 \equiv \frac{\phi_2^2}{\sigma_2^2} + \frac{\phi_3^2}{\sigma_3^2} = 1$ confined to the plane $\phi_1 = 0$. Substituting this condition in (11), the following eight solutions, connecting B and C , are obtained:

$$\bar{\phi}_1(x) = 0; \quad \bar{\phi}_2(x) = \frac{(-1)^\alpha \bar{\sigma}_2}{\sqrt{1 + e^{-2\sqrt{2}\sigma_2^2 x}}}; \quad \bar{\phi}_3(x) = \frac{(-1)^\beta \bar{\sigma}_3}{\sqrt{1 + e^{2\sqrt{2}\sigma_3^2 x}}} \quad (17)$$

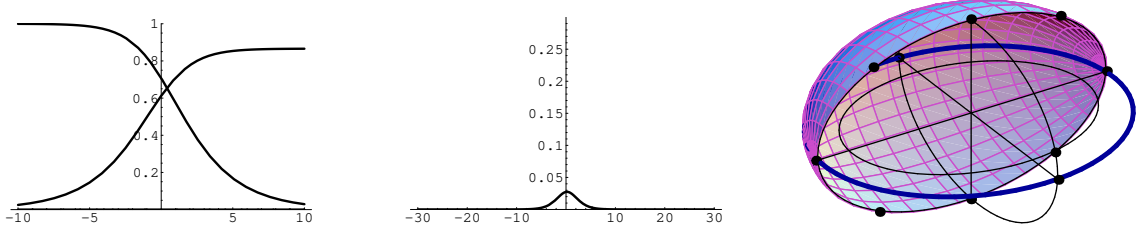


Figure 3: Kink form factor (a), energy density (b) and orbits (c) for K_1^{CD} kinks.

with $\alpha, \beta, \delta = 0, 1$. Again the non-null components, ϕ_2 and ϕ_3 in this case, are kink shaped. In Figure 4(a) a K_1^{BC} kink is represented for $\alpha = \beta = \delta = 0$. The analogous trajectory leaves the instability point B_+ of $U = -V$ “at” $x = -\infty$ and arrives at another instability point C_+ “at” $x = \infty$. These solutions are made of a single lump and carry energy equal to $E(K_1^{BC}) = \frac{\bar{\sigma}_2^4 - \bar{\sigma}_3^4}{2\sqrt{2}}$, a function of both coupling constants.

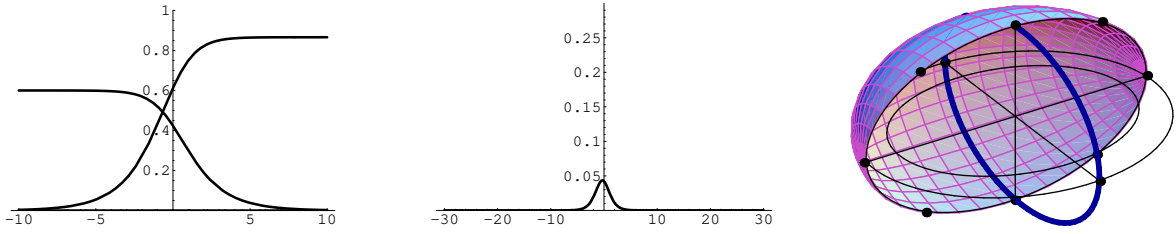


Figure 4: Kink form factor (a), energy density (b) and orbits (c) for K_1^{BC} kinks.

In sum, there exist three kinds of one-body solitary waves or basic extended particles, denoted as K_1^{CD} , K_1^{OB} and K_1^{BC} . The energy of K_1^{CD} increases as the eccentricity of the ellipse e_3 grows, whereas the energy of K_1^{OB} decreases when the eccentricity of e_2 increases. The energy for the K_1^{BC} lumps depends on the difference of the eccentricity of the ellipses e_3 and e_2 and becomes zero when these magnitudes are equal. Which basic particle is more energetic depends on the values of the coupling constants σ_2 and σ_3 . The figures in this paper have been drawn for the values $\sigma_2 = 0.5$ and $\sigma_3 = 0.8$.

3.2 Two-body solitary waves

1. $K_2^{OC}(b)$: We shall now tackle the search for solutions in the $\phi_1 = 0$ plane, $\nu = 1$ in elliptic coordinates, see Figure 5(c). The Hamiltonian (14) restricted to this plane reads

$$H = \frac{2P_3(\lambda)p_\lambda^2 + P_4(\lambda)}{(\lambda - \mu)(\lambda - 1)} + \frac{2P_3(\mu)p_\mu^2 + P_4(\mu)}{(\mu - \lambda)(\mu - 1)}$$

The standard Hamilton-Jacobi procedure prescribes how to solve the HJ equation

$$\frac{\partial \mathcal{S}}{\partial x} + H\left(\frac{\partial \mathcal{S}}{\partial \lambda}, \frac{\partial \mathcal{S}}{\partial \mu}, \lambda, \mu\right) = 0$$

assuming the separable form of the Hamilton’s principal function $\mathcal{S} = \mathcal{S}_x + \mathcal{S}_\lambda(\lambda) + \mathcal{S}_\mu(\mu)$. The PDE HJ equation becomes a ODE system and the complete integral can be found by quadratures

$$\mathcal{S}_x = -Ex; \quad \mathcal{S}_\lambda = s_\lambda \int d\lambda \sqrt{\frac{F - \frac{1}{2}E\lambda}{(\bar{\sigma}_2^2 - \lambda)(\bar{\sigma}_3^2 - \lambda)} + \frac{\lambda^2}{2}}; \quad \mathcal{S}_\mu = s_\mu \int d\mu \sqrt{\frac{F - \frac{1}{2}E\mu}{(\bar{\sigma}_2^2 - \mu)(\bar{\sigma}_3^2 - \mu)} + \frac{\mu^2}{2}}$$

in terms of the integration constants E, F . $s_i = \text{Sign } p_i$ denote the sign of the momenta.

The trajectories are determined from the orbits selected by the equation $\gamma_2 = \frac{\partial \mathcal{S}}{\partial F}$ where γ_2 is a constant, and the time-schedule fixed by the equation $\gamma_1 = \frac{\partial \mathcal{S}}{\partial E}$ where γ_1 is another arbitrary constant. The asymptotic conditions (7) picking finite action trajectories force $E = F = 0$. The finite action trajectories of the analogous mechanical problem are thus determined by the pair of equations

$$e^{\sqrt{2}\gamma_2} = \left[\frac{\lambda \frac{1}{\bar{\sigma}_2^2 \bar{\sigma}_3^2} (\bar{\sigma}_2^2 - \lambda) \frac{1}{\bar{\sigma}_2^2 \bar{\sigma}_3^2}}{(\bar{\sigma}_3^2 - \lambda) \frac{1}{\bar{\sigma}_3^2 \bar{\sigma}_3^2}} \right]^{s_\lambda} \left[\frac{\mu \frac{1}{\bar{\sigma}_2^2 \bar{\sigma}_3^2} (\mu - \bar{\sigma}_2^2) \frac{1}{\bar{\sigma}_2^2 \bar{\sigma}_3^2}}{(\bar{\sigma}_3^2 - \mu) \frac{1}{\bar{\sigma}_3^2 \bar{\sigma}_3^2}} \right]^{s_\mu}; \quad e^{2\sqrt{2}\sigma_{32}^2 \bar{x}} = \left[\frac{\bar{\sigma}_2^2 - \lambda}{\bar{\sigma}_3^2 - \lambda} \right]^{s_\lambda} \left[\frac{\bar{\sigma}_2^2 - \mu}{\mu - \bar{\sigma}_3^2} \right]^{s_\mu}$$

which can be reshuffled in the form:

$$e^{-\sqrt{2}\bar{\sigma}_2^2(2\bar{x} - \bar{\sigma}_3^2 \gamma_2)} = \left[\frac{\lambda}{\bar{\sigma}_2^2 - \lambda} \right]^{s_\lambda} \left[\frac{\mu}{\bar{\sigma}_2^2 - \mu} \right]^{s_\mu}; \quad e^{-\sqrt{2}\bar{\sigma}_3^2(2\bar{x} - \bar{\sigma}_2^2 \gamma_2)} = \left[\frac{\lambda}{\bar{\sigma}_3^2 - \lambda} \right]^{s_\lambda} \left[\frac{\mu}{\mu - \bar{\sigma}_3^2} \right]^{s_\mu} \quad (18)$$

The choice $s_\lambda = s_\mu$ in (18) yields solutions in the topological sector \mathcal{C}^{OC} . Translating (18) back to Cartesian coordinates, we obtain the following field profiles for the associated one-parametric family of solitary waves parametrized by $b^2 = e^{-\sqrt{2}\sigma_{32}^2 \bar{\sigma}_3^2 \gamma_2}$:

$$\bar{\phi}_1 = 0; \quad \bar{\phi}_2 = \frac{(-1)^\alpha \bar{\sigma}_2}{\sqrt{1 + \frac{\sigma_{32}^2}{\bar{\sigma}_3^2} e^{-2\sqrt{2}\bar{\sigma}_2^2 \bar{x}} + \frac{\bar{\sigma}_2^2}{\bar{\sigma}_3^2} b^2 e^{-2\sqrt{2}\bar{\sigma}_3^2 \bar{x}}}}; \quad \bar{\phi}_3 = \frac{b \bar{\sigma}_3}{\sqrt{b^2 + \frac{\sigma_{32}^2}{\bar{\sigma}_2^2} e^{-2\sqrt{2}\bar{\sigma}_3^2 \bar{x}} + \frac{\bar{\sigma}_3^2}{\bar{\sigma}_2^2} e^{2\sqrt{2}\bar{\sigma}_3^2 \bar{x}}}} \quad (19)$$

We refer to these solutions as $K_2^{OC}(b)$ because they are made of two basic lumps. $\alpha = 0$ describes solutions joining O and C^+ whereas $\alpha = 1$ gives solitary waves which connect the points O and C^- . In Figure 5(a) a K_2^{OC} kink with $\alpha = \gamma = 0$ is depicted. The analogous trajectory departs from O and arrives at C_+ as x goes from $-\infty$ to ∞ .

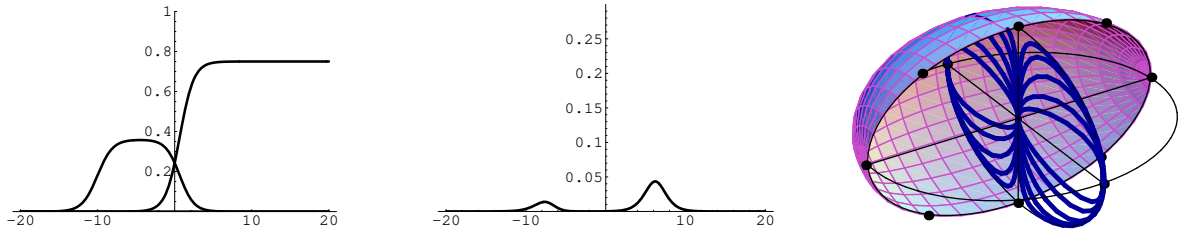


Figure 5: Kink form factor (a), energy density (b) and orbits (c) for $K_2^{OC}(b)$ kinks.

One of the non-null components, ϕ_2 , is again of kink form but the other, ϕ_3 is bell-shaped. The energy density is localized at two different points, i.e. this kind of kinks are formed by two basic lumps and are two-body solitary waves. They are made from one K_1^{OB} and one K_1^{BC} kink, although due to the nonlinearity of (19) the composition is much more intricate than the simple sum of expressions (15) and (17). The value of b determines the distance between these lumps; if $b = 0$, the centers of the one-body solitary waves coincide [14] and they are superposed. Moreover,

$$E[K_2^{OC}(b)] = E(K_1^{OB}) + E(K_1^{BC}) = \frac{\bar{\sigma}_2^4}{2\sqrt{2}} \quad .$$

The energy depends on the eccentricity of the ellipse e_3 . We remark that the fact of finding the combination of one K_1^{OB} and one K_1^{BC} as static solutions of (5) means that there are no forces between these basic particles when they are at rest or their relative velocity is zero. The singular member $K_2^{OC}(0)$ is located on the ϕ_2 axis between the points C_+ and C_- .

2. $K_2^{BD}(b)$: On the ellipsoid $E \equiv \phi_1^2 + \frac{\phi_2^2}{\sigma_2^2} + \frac{\phi_3^2}{\sigma_3^2} = 1$, or $\lambda = 0$, the Hamiltonian (14) and the Hamilton-Jacobi equation reads:

$$H = \frac{2P_3(\mu)p_\mu^2 + P_4(\mu)}{\mu(\mu - \nu)} + \frac{2P_3(\nu)p_\nu^2 + P_4(\nu)}{\nu(\nu - \mu)}, \quad \frac{\partial \mathcal{S}}{\partial x} + H \left(\frac{\partial \mathcal{S}}{\partial \mu}, \frac{\partial \mathcal{S}}{\partial \nu}, \mu, \nu \right) = 0 \quad . \quad (20)$$

Separation of variables $\mathcal{S} = \mathcal{S}_x(x) + \mathcal{S}_\lambda(\lambda) + \mathcal{S}_\mu(\mu)$ affords the solution of (20) for the Hamilton principal function via quadratures: $\mathcal{S}_x = -Ex$,

$$\mathcal{S}_\mu = s_\mu \int d\mu \sqrt{\frac{(F + \frac{1}{2}E\mu)\mu}{(1-\mu)(\bar{\sigma}_2^2 - \mu)(\bar{\sigma}_3^2 - \mu)} + \frac{\mu^2}{2}}; \quad \mathcal{S}_\nu = s_\nu \int d\nu \sqrt{\frac{(F + \frac{1}{2}E\nu)\nu}{(1-\nu)(\bar{\sigma}_2^2 - \nu)(\bar{\sigma}_3^2 - \nu)} + \frac{\nu^2}{2}},$$

if E and F are the separation constants. The finite action trajectories, $E = F = 0$, are determined by:

1. Orbits

$$\gamma_2 = \frac{\partial \mathcal{S}}{\partial F} \quad \Leftrightarrow \quad e^{\sqrt{2}\sigma_{32}^2 \gamma_2} = \left[\frac{(\bar{\sigma}_2^2 - \mu)^{\frac{1}{\sigma_2^2}}}{(1-\mu)^{\frac{1}{\sigma_2^2} - \frac{1}{\sigma_3^2}} (\mu - \bar{\sigma}_3^2)^{\frac{1}{\sigma_3^2}}} \right]^{s_\mu} \left[\frac{(\nu - \bar{\sigma}_2^2)^{\frac{1}{\sigma_2^2}}}{(1-\nu)^{\frac{1}{\sigma_2^2} - \frac{1}{\sigma_3^2}} (\nu - \bar{\sigma}_3^2)^{\frac{1}{\sigma_3^2}}} \right]^{s_\nu}$$

2. Time schedules

$$\gamma_1 = \frac{\partial \mathcal{S}}{\partial E} \quad \Leftrightarrow \quad e^{2\sqrt{2}\sigma_{32}^2 \bar{x}} = \left[\frac{(\bar{\sigma}_2^2 - \mu)^{\frac{1-\sigma_2^2}{\sigma_2^2}}}{(1-\mu)^{\frac{1}{\sigma_2^2} - \frac{1}{\sigma_3^2}} (\mu - \bar{\sigma}_3^2)^{\frac{1-\sigma_3^2}{\sigma_3^2}}} \right]^{s_\mu} \left[\frac{(\nu - \bar{\sigma}_2^2)^{\frac{1-\sigma_2^2}{\sigma_2^2}}}{(1-\nu)^{\frac{1}{\sigma_2^2} - \frac{1}{\sigma_3^2}} (\nu - \bar{\sigma}_3^2)^{\frac{1-\sigma_3^2}{\sigma_3^2}}} \right]^{s_\nu}$$

In the field theoretical problem, the time schedule becomes the kink form factor.

It is convenient to rearrange the above expressions and write:

$$e^{\sqrt{2}\sigma_2^2(\bar{\sigma}_3^2 \gamma_2 - 2\bar{x})} = \left[\frac{1-\mu}{\bar{\sigma}_2^2 - \mu} \right]^{s_\mu} \left[\frac{1-\nu}{\nu - \bar{\sigma}_2^2} \right]^{s_\nu}; \quad e^{\sqrt{2}\sigma_3^2(\bar{\sigma}_2^2 \gamma_2 - 2\bar{x})} = \left[\frac{1-\mu}{\mu - \bar{\sigma}_3^2} \right]^{s_\mu} \left[\frac{1-\nu}{\nu - \bar{\sigma}_3^2} \right]^{s_\nu} \quad . \quad (21)$$

Choosing $s_\mu = s_\nu$ in (21), solitary waves living in in the topological sector \mathcal{C}^{OC} are obtained. Back in Cartesian coordinates we find:

$$\begin{aligned} \bar{\phi}_1(x; b) &= \frac{(-1)^\alpha}{\sqrt{1 + \frac{\sigma_2^2}{\sigma_{32}^2} e^{2\sqrt{2}\sigma_3^2 x} + \frac{\sigma_3^2}{\sigma_{32}^2} b^2 e^{2\sqrt{2}\sigma_2^2 x}}} \\ \bar{\phi}_2(x; b) &= \frac{b}{\sqrt{b^2 + \frac{\sigma_2^2}{\sigma_3^2} e^{2\sqrt{2}\sigma_{32}^2 x} + \frac{\sigma_{32}^2}{\sigma_3^2} e^{-2\sqrt{2}\sigma_2^2 x}}} \\ \bar{\phi}_3(x; b) &= \frac{(-1)^\beta}{\sqrt{1 + \frac{\sigma_{32}^2}{\sigma_2^2} e^{-2\sqrt{2}\sigma_3^2 x} + \frac{\sigma_3^2}{\sigma_2^2} b^2 e^{-2\sqrt{2}\sigma_{32}^2 x}}} \end{aligned} \quad . \quad (22)$$

$\alpha, \beta = 0, 1$ determine the quadrant of the ellipsoid delimited by the $\phi_1 = 0$ and $\phi_3 = 0$ planes where the solutions are confined, see Figure 6(c). Again, this is a one-parametric family of solitary waves, denoted as $K_2^{DB}(b)$. An $\alpha = \beta = 0$ member of this family is depicted in Figure 6(c), asymptotically connecting the points D_+ and B_+ . Note that these solitary waves have two kink-shaped non-null components and the third one is bell-shaped. The energy density, however, shows two basic lumps, one K_1^{BC} and one

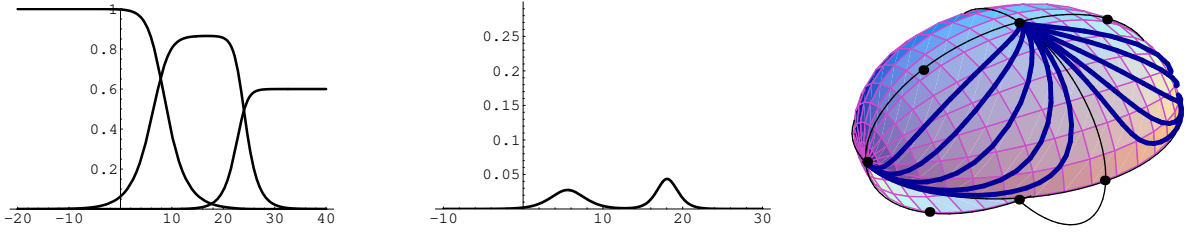


Figure 6: Form factor (a), energy density (b) and orbits (c) for K_2^{BD} kinks.

K_1^{CD} , a composition pointing to lack of interaction between these particles at rest. The energy of these two-body kinks depends on the eccentricity of the ellipse e_2 ,

$$E[K_2^{BD}(b)] = E(K_1^{BC}) + E(K_1^{CD}) = \frac{\sigma_3^2(2 - \sigma_3^2)}{2\sqrt{2}}$$

The $K_2^{BD}(0)$ kink orbit is the ellipse e_2 ; for $b = 0$ $E(K_1^{BC})$ and $E(K_1^{CD})$ are superposed, see [14].

In sum, there are two kinds of static two-body solitary waves formed by either a K_1^{OB} plus a K_1^{BC} kinks or a K_1^{BC} plus K_1^{CD} lumps. We remark that there is no static configurations involving a K_1^{OB} and K_1^{CD} kinks or two particles of the same kind. Thus, these particles interact one with each other.

3.3 Three-body solitary waves

1. $K_3^{OD}(a, b)$: The Hamilton-Jacobi equation

$$\frac{\partial \mathcal{S}}{\partial x} + H\left(\frac{\partial \mathcal{S}}{\partial \lambda}, \frac{\partial \mathcal{S}}{\partial \mu}, \frac{\partial \mathcal{S}}{\partial \nu}, \lambda, \mu, \nu\right) = 0$$

for the complete Hamiltonian (14) of the analogous mechanical system is in any case separable. Writing the Hamilton principal function in the form $\mathcal{S} = -Ex + \mathcal{S}_\lambda + \mathcal{S}_\mu + \mathcal{S}_\nu$, one is led to the quadratures:

$$\begin{aligned} \mathcal{S}_\lambda &= s_\lambda \int \sqrt{\frac{E\lambda^2 + F_1\lambda + F_3}{2(1-\lambda)(\bar{\sigma}_2^2 - \lambda)(\bar{\sigma}_3^2 - \lambda)} + \frac{\lambda^2}{2}} d\lambda \\ \mathcal{S}_\mu &= s_\mu \int \sqrt{\frac{E\mu^2 + F_1\mu + F_2}{2(1-\mu)(\bar{\sigma}_2^2 - \mu)(\bar{\sigma}_3^2 - \mu)} + \frac{\mu^2}{2}} d\mu \\ \mathcal{S}_\nu &= s_\nu \int \sqrt{\frac{E\nu^2 + F_1\nu + F_2}{2(1-\nu)(\bar{\sigma}_2^2 - \nu)(\bar{\sigma}_3^2 - \nu)} + \frac{\nu^2}{2}} d\nu \end{aligned}$$

Again, finite action trajectories $E = F_1 = F_2 = 0$ are determined by:

1. Orbits, given by the intersection of two surfaces in $P(0)$.

1a. $\gamma_2 = \frac{\partial \mathcal{S}}{\partial F_1}$, or,

$$e^{2\sqrt{2}\sigma_{32}\gamma_2} = \left[\frac{(\bar{\sigma}_2^2 - \lambda)^{\frac{1}{\sigma_2^2}}}{(1-\lambda)^{\frac{\sigma_{32}^2}{\sigma_2^2\sigma_3^2}} (\bar{\sigma}_3^2 - \lambda)^{\frac{1}{\sigma_3^2}}} \right]^{s_\lambda} \left[\frac{(\bar{\sigma}_2^2 - \mu)^{\frac{1}{\sigma_2^2}}}{(1-\mu)^{\frac{\sigma_{32}^2}{\sigma_2^2\sigma_3^2}} (\mu - \bar{\sigma}_3^2)^{\frac{1}{\sigma_3^2}}} \right]^{s_\mu} \left[\frac{(\nu - \bar{\sigma}_2^2)^{\frac{1}{\sigma_2^2}}}{(1-\nu)^{\frac{\sigma_{32}^2}{\sigma_2^2\sigma_3^2}} (\nu - \bar{\sigma}_3^2)^{\frac{1}{\sigma_3^2}}} \right]^{s_\nu}$$

1b. $\gamma_3 = \frac{\partial \mathcal{S}}{\partial F_2}$, or,

$$e^{2\sqrt{2}\sigma_{32}^2\gamma_3} = \left[\frac{\lambda \frac{\sigma_{32}^2}{\sigma_2^2\sigma_3^2} (\bar{\sigma}_2^2 - \lambda) \frac{1}{\sigma_2^2\sigma_2^2}}{(1-\lambda) \frac{\sigma_{32}^2}{\sigma_2^2\sigma_3^2} (\bar{\sigma}_3^2 - \lambda) \frac{1}{\sigma_3^2\sigma_3^2}} \right]^{s_\lambda} \left[\frac{\mu \frac{\sigma_{32}^2}{\sigma_2^2\sigma_3^2} (\bar{\sigma}_2^2 - \mu) \frac{1}{\sigma_2^2\sigma_2^2}}{(1-\mu) \frac{\sigma_{32}^2}{\sigma_2^2\sigma_3^2} (\mu - \bar{\sigma}_3^2) \frac{1}{\sigma_3^2\sigma_3^2}} \right]^{s_\mu} \left[\frac{\nu \frac{\sigma_{32}^2}{\sigma_2^2\sigma_3^2} (\nu - \bar{\sigma}_2^2) \frac{1}{\sigma_2^2\sigma_2^2}}{(1-\nu) \frac{\sigma_{32}^2}{\sigma_2^2\sigma_3^2} (\nu - \bar{\sigma}_3^2) \frac{1}{\sigma_3^2\sigma_3^2}} \right]^{s_\nu}$$

2. Time schedules, or kink form factor: $\gamma_1 = \frac{\partial \mathcal{S}}{\partial E}$, or,

$$e^{2\sqrt{2}\sigma_{32}^2\bar{x}} = \left[\frac{(\bar{\sigma}_2^2 - \lambda) \frac{\sigma_2^2}{\sigma_2^2}}{(1-\lambda) \frac{\sigma_{32}^2}{\sigma_2^2\sigma_3^2} (\bar{\sigma}_3^2 - \lambda) \frac{\sigma_3^2}{\sigma_3^2}} \right]^{s_\lambda} \left[\frac{(\bar{\sigma}_2^2 - \mu) \frac{\sigma_2^2}{\sigma_2^2}}{(1-\mu) \frac{\sigma_{32}^2}{\sigma_2^2\sigma_3^2} (\mu - \bar{\sigma}_3^2) \frac{\sigma_3^2}{\sigma_3^2}} \right]^{s_\mu} \left[\frac{(\nu - \bar{\sigma}_2^2) \frac{\sigma_2^2}{\sigma_2^2}}{(1-\nu) \frac{\sigma_{32}^2}{\sigma_2^2\sigma_3^2} (\nu - \bar{\sigma}_3^2) \frac{\sigma_3^2}{\sigma_3^2}} \right]^{s_\nu}$$

These expressions are conveniently rearranged in the simpler form:

$$\begin{aligned} \left[\frac{\lambda}{1-\lambda} \right]^{s_\lambda} \left[\frac{\mu}{1-\mu} \right]^{s_\mu} \left[\frac{\nu}{1-\nu} \right]^{s_\nu} &= e^{2\sqrt{2}(x-(\bar{\sigma}_2^2+\bar{\sigma}_3^2)\gamma_2+\bar{\sigma}_2^2\bar{\sigma}_3^2\gamma_3)} \\ \left[\frac{\lambda}{\bar{\sigma}_2^2-\lambda} \right]^{s_\lambda} \left[\frac{\mu}{\bar{\sigma}_2^2-\mu} \right]^{s_\mu} \left[\frac{\nu}{\nu-\bar{\sigma}_2^2} \right]^{s_\nu} &= e^{2\sqrt{2}\bar{\sigma}_2^2(x-(2-\bar{\sigma}_3^2)\gamma_2+\bar{\sigma}_3^2\gamma_3)} \\ \left[\frac{\lambda}{\bar{\sigma}_3^2-\lambda} \right]^{s_\lambda} \left[\frac{\mu}{\mu-\bar{\sigma}_3^2} \right]^{s_\mu} \left[\frac{\nu}{\nu-\bar{\sigma}_3^2} \right]^{s_\nu} &= e^{2\sqrt{2}\bar{\sigma}_3^2(x-(2-\bar{\sigma}_2^2)\gamma_2+\bar{\sigma}_2^2\gamma_3)} \end{aligned} \quad (23)$$

Choosing $s_\lambda = s_\mu = s_\nu = 1$ in (23) we obtain, back in Cartesian coordinates, the two-parametric family of solitary waves, denoted as $K_3^{OD}(a, b)$:

$$\begin{aligned} \bar{\phi}_1(x; a, b) &= \frac{(-1)^\alpha}{\sqrt{1 + \frac{\sigma_2^2\sigma_3^2}{\sigma_2^2\sigma_3^2} e^{2\sqrt{2}\bar{x}} + \frac{\sigma_2^2}{\sigma_3^2} b^2 e^{2\sqrt{2}\sigma_3^2\bar{x}} + \frac{\sigma_3^2}{\sigma_2^2} a^2 e^{2\sqrt{2}\sigma_2^2\bar{x}}}} \\ \bar{\phi}_2(x; a, b) &= \frac{a}{\sqrt{\frac{a^2}{\sigma_2^2} + \frac{\sigma_2^2}{\sigma_2^2\sigma_3^2} e^{2\sqrt{2}\bar{\sigma}_2^2\bar{x}} + \frac{1}{\sigma_3^2} e^{-2\sqrt{2}\sigma_2^2\bar{x}} + \frac{\sigma_2^2}{\sigma_3^2\sigma_3^2} b^2 e^{2\sqrt{2}\sigma_3^2\bar{x}}}} \\ \bar{\phi}_3(x; a, b) &= \frac{b}{\sqrt{\frac{b^2}{\sigma_3^2} + \frac{\sigma_3^2}{\sigma_2^2\sigma_3^2} e^{2\sqrt{2}\bar{\sigma}_3^2\bar{x}} + \frac{1}{\sigma_2^2} e^{-2\sqrt{2}\sigma_3^2\bar{x}} + \frac{\sigma_3^2}{\sigma_2^2\sigma_2^2} a^2 e^{-2\sqrt{2}\sigma_2^2\bar{x}}}} \end{aligned} \quad (24)$$

Without counting the center of the kinks, related to γ_1 , these kinks depend generically on two parameters a and b , defined respectively in terms of γ_2 and γ_3 as: $\sigma_{32}^2 a^2 = e^{-2\sqrt{2}\sigma_2^2\sigma_{32}^2\gamma_2}$, $\sigma_{32}^2 b^2 = e^{-2\sqrt{2}\sigma_3^2\sigma_{32}^2\gamma_3}$. Additionally, $\alpha = 0$ or 1 specifies in which semi-space $\phi_1 > 0$ or $\phi_1 < 0$ these solutions live, see Figure 7(c). In Figure 7(a) a K_3^{OD} kink orbit is plotted for $\alpha = 0$. The particle leaves the point D_+ at $x = -\infty$ and arrives in O at $x = +\infty$, tracing a orbit confined to be in a octant of the interior of the ellipsoid E . The associated solitary wave thus lives in the \mathcal{C}^{OD+} sector of the configuration space and has one kink-like and two bell-shaped components. The energy density of a solitary wave like this is composed of three lumps: the basic particles K_1^{OB} , K_1^{BC} and K_1^{CD} , see Figure 7(b).

The energy of any kink solution of the (24) family is topological and does not depend neither on the (a, b) parameters nor on the coupling constants:

$$\begin{aligned} E[K_3^{OD}(a, b)] &= |W(\bar{\phi}_1(\infty; a, b), \bar{\phi}_2(\infty; a, b), \bar{\phi}_3(\infty; a, b)) - W(\bar{\phi}_1(-\infty; a, b), \bar{\phi}_2(-\infty; a, b), \bar{\phi}_3(-\infty; a, b))| \\ &= E(K_1^{OB}) + E(K_1^{BC}) + E(K_1^{CD}) = \frac{1}{2\sqrt{2}} \end{aligned}$$

shows degeneracy in energy and a curious kink energy sum rule.

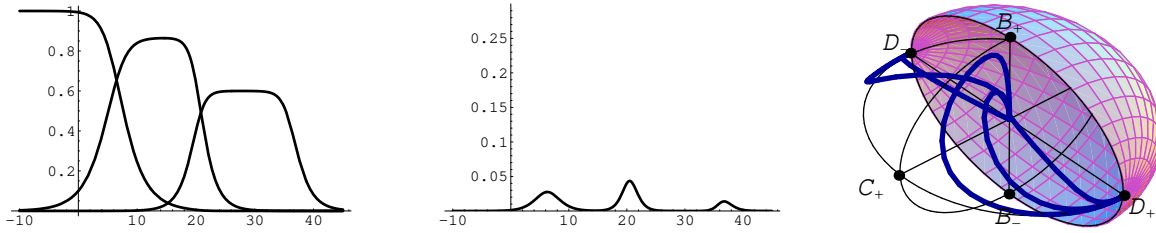


Figure 7: *Kink form factor (a), energy density (b), and orbits (c) for $K_3^{OD}(a, b)$ kinks.*

The choice of the parameters a and b to draw Figure 7 aims at identifying the basic components of any $K_3^{OD}(a, b)$ kink. In general, the parameter a is set in order to find kinks in the $\phi_3 = 0$ plane for $a = 0$, whereas the parameter b runs through \mathbb{R} . In Figure 8(c) several orbits of the $K_3^{OD}(0, b)$ kink sub-family are shown. Apparently these solutions are made of two lumps, as illustrated in Figure 8(b). The paradox is fictitious because the K_1^{BC} and K_1^{OB} lumps are superposed for all the members of this sub-family. Therefore, these kinks also involve the three basic particles and we recognize a as the measure of the distance between K_1^{BC} and K_1^{OB} .

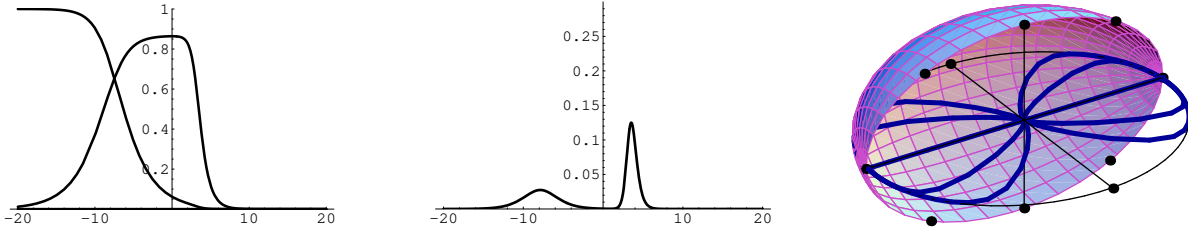


Figure 8: *Form factor (a), energy density (b) and orbits (c) for $K_3^{OD}(0, b)$ kinks.*

In the same vein, $K_3^{OD}(a, 0)$ solitary waves live in the plane $\phi_2 = 0$. Each member of the $b = 0$ family displays two lumps, one K_1^{OB} kink and a superposition of a K_1^{BC} and a K_1^{CD} basic particles. b thus measures the distance between the K_1^{BC} and K_1^{CD} basic kinks. There exists a member of the family in the intersection of the two sub-families, i.e., the $K_3^{OD}(0, 0)$ kink, whose orbit lies on the ϕ_1 axis. Generically, the $K_3(a, b)$ solitary waves are three-body kinks, but in the $K_3(0, 0)$ configuration the three particles or lumps are completely fused. In Figure 9 the energy density of $K_3(10, b)$ solitary waves is depicted for several values of the parameter b . A similar pattern would be observed by setting the value of b to be constant and letting the value of a vary, although the rôle of the basic particles would be swapped.

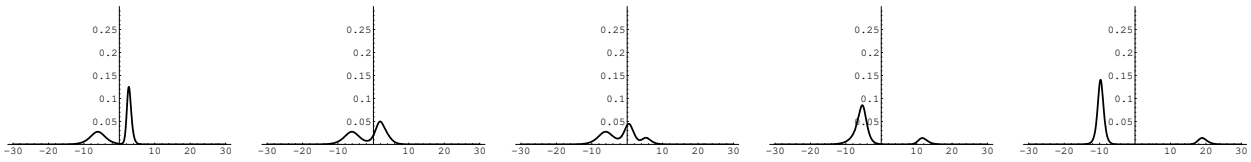


Figure 9: *Energy Density for $K_3^{OD}(10, b)$ kinks: a) $b = 0$, Green zone B, b) $b = 5$, Green zone B, c) $b = 10$, Blue zone D, d) $b = 240$, Green zone C, and e) $b = 10000$, Green zone C. All the colored zones are shown in Figure 10.*

It is interesting to remark that the choice of signs, providing the solutions (24), is such that the inverse image of

$$s_\lambda S_\lambda(\lambda) + s_\mu S_\mu(\mu) + s_\nu S_\nu(\nu)$$

in the coordinate transformation (13) is the Hamilton characteristic function in \mathbb{R}^3 :

$$W(\phi_1, \phi_2, \phi_3) = \frac{1}{\sqrt{8}} [(\phi_1^2 + \phi_2^2 + \phi_3^2 - 1)^2 + 2\sigma_2^2 \phi_2^2 + 2\sigma_3^2 \phi_3^2] \quad . \quad (25)$$

Thus,

- (24) are the gradient flow lines of $W(\phi_1, \phi_2, \phi_3)$:

$$\frac{d\phi_1}{dx} = \mp \frac{\partial W}{\partial \phi_1} \quad , \quad \frac{d\phi_2}{dx} = \mp \frac{\partial W}{\partial \phi_2} \quad , \quad \frac{d\phi_3}{dx} = \mp \frac{\partial W}{\partial \phi_3} \quad . \quad (26)$$

The ODE system (26) is separable and tantamount to (23) in elliptic coordinates.

- $W(\phi_1, \phi_2, \phi_3)$ is no more than the potential energy of a very well known integrable system: the Garnier system, the analogous mechanical system of the field theoretical model discussed in [23] and [24]. Our model is chosen in such a way that the potential energy of the mechanical analogous system is the square of the norm of the gradient of the potential energy of the Garnier system. No wonder integrability is found!

In sum, there exist three-body solitary wave solutions that are static configurations formed by the three kinds of basic particles, with no forces between lumps.

3.3.1 The moduli space of three-body kinks

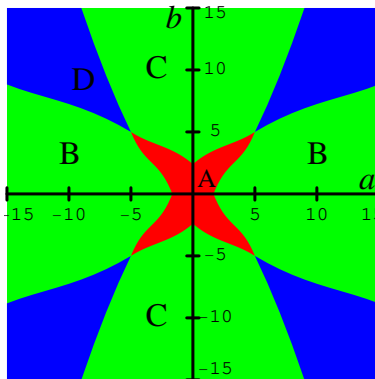


Figure 10: *Tiling of the moduli space according to the number of lumps.*

To make these statements more precise, we need a better understanding of the physical meaning of the (a, b) coordinates parametrizing the moduli space of K_3 solitary waves. To achieve this goal, the number of lumps should be identified with the number of maxima of the energy density of the K_3 solution on the line. For instance, in the $\sigma_3^2 = 2\sigma_2^2 = \frac{1}{3}$ case, the energy density reads:

$$\mathcal{E}_K(z) = \frac{2z(2a^2 + (3a^4 + 4b^2)z + 12a^2b^2z^2 + (10a^2 + a^4b^2 + 12b^4)z^3 + (32b^2 + 2a^2b^4)z^4 + (27 + 6a^2b^2)z^5 + 8a^2z^6 + b^2z^7)}{27(1 + a^2z + b^2z^2 + z^3)^3},$$

where $z = e^{\frac{2\sqrt{2}x}{3}}$. It is not possible to find analytically the extremal points of $\mathcal{E}_K(z)$ because one should find the roots of a sixth order polynomial as a function of a and b . Solutions of the equation

$$\frac{\partial \mathcal{E}_K}{\partial z}(z, a, b) = 0 \quad , \quad (27)$$

however, can be studied numerically. We find the following pattern in different ranges of a and b :

- There is a single real solution of (27) in the A domain of the moduli space, see Figure 10. The solution is a maximum of $\varepsilon_K(z, a, b)$ and the three lumps are glued together.

- In the two B domains there are three real solutions to equation (27); two of them are maxima and the remaining one is a minimum of $\varepsilon_K(z, a, b)$. All over these regions of the moduli space K_1^{CD} and K_1^{BC} sit on top of each other, whereas K_1^{OB} is apart.
- Also in the two C domains there are three real solutions, two maxima and one minimum, but now only K_1^{CD} is separated.
- Finally, in the four D domains there are five real solutions of (27), three of which are maxima and the other two are minima of the energy density, and the three basic kinks are totally split apart from each other .

3.4 Four-body solitary waves

1. $K_4^{BB}(b)$: The sign combinations $s_\lambda \neq s_\mu$ in the (18) system of equations offer a one-parametric family of solutions belonging to the \mathcal{C}^{BB} topological sectors and confined to living in the $\phi_1 = 0$ plane. The Cartesian field profiles are:

$$\begin{aligned}\bar{\phi}_1(x) &= 0 \\ \bar{\phi}_2(x) &= \frac{(-1)^\alpha \bar{\sigma}_2^2 \sigma_{32} (1 + e^b e^{-2\sqrt{2}\bar{\sigma}_3^2 \bar{x}})}{(\bar{\sigma}_2^2 + \sigma_{32}^2 e^b e^{-2\sqrt{2}\bar{\sigma}_3^2 \bar{x}} + \bar{\sigma}_3^2 e^b e^{2\sqrt{2}\sigma_{32}^2 \bar{x}})^{\frac{1}{2}} (\bar{\sigma}_{32}^2 + \bar{\sigma}_2^2 e^b e^{-2\sqrt{2}\bar{\sigma}_3^2 \bar{x}} + \bar{\sigma}_3^2 e^{-2\sqrt{2}\bar{\sigma}_2^2 \bar{x}})^{\frac{1}{2}}} \\ \bar{\phi}_3(x) &= \frac{\bar{\sigma}_3^2 \sigma_{32} (1 - e^{-2\sqrt{2}\bar{\sigma}_2^2 \bar{x}})}{(\bar{\sigma}_3^2 + \sigma_{32}^2 e^{-2\sqrt{2}\bar{\sigma}_2^2 \bar{x}} + \bar{\sigma}_2^2 e^{-b} e^{-2\sqrt{2}\sigma_{32}^2 \bar{x}})^{\frac{1}{2}} (\bar{\sigma}_{32}^2 + \bar{\sigma}_2^2 e^b e^{-2\sqrt{2}\bar{\sigma}_3^2 \bar{x}} + \bar{\sigma}_3^2 e^{-2\sqrt{2}\bar{\sigma}_2^2 \bar{x}})^{\frac{1}{2}}}\end{aligned}$$

Again, $b \in \mathbb{R}$ is a real parameter and $\alpha = 0, 1$. In Figure 11(a) a $K_4^{BB}(b)$ kink is represented: the second component is bell-shaped but $\bar{\phi}_3(x)$ is formed by two kinks. The kink trajectory departs from the point B_- and arrives in B_+ when x goes from $-\infty$ to ∞ , crossing through the focus F_1 of the ellipse e_1 . Indeed, this behavior is general and the trajectory of each member $K_4^{BB}(b)$ passes through F_1 at the same “time” $\bar{x} = 0$, see Figure 11(c). In Figure 11(b), the energy density is plotted, showing the structure of this kind of solitary wave solutions: these kinks are composed of three lumps; two of them are easily recognizable as the basic particles K_1^{OB} and K_1^{BC} . The other kink is located between the previous ones and has the same energy as the sum of the energy of the two basic particles. Later stability analysis will show the lump in the middle decaying to the K_1^{OB} and K_1^{BC} one-body kinks, but exactly superposed in $K_2^{OC}(0)$ they are in unstable equilibrium. In any case, the $K_4^{BB}(b)$ solutions are made of four one-body kinks: two K_1^{OB} 's and two K_1^{BC} 's. The energy of these solutions is:

$$E[K_4^{BB}(b)] = E(K_1^{BO}) + E[K_2^{OC}(0)] + E(K_1^{BC}) = 2E(K_1^{OB}) + 2E(K_1^{BC}) = \frac{\bar{\sigma}_2^4}{\sqrt{2}} .$$

An interesting point should be noticed: we claimed that the presence of two particles of the same kind

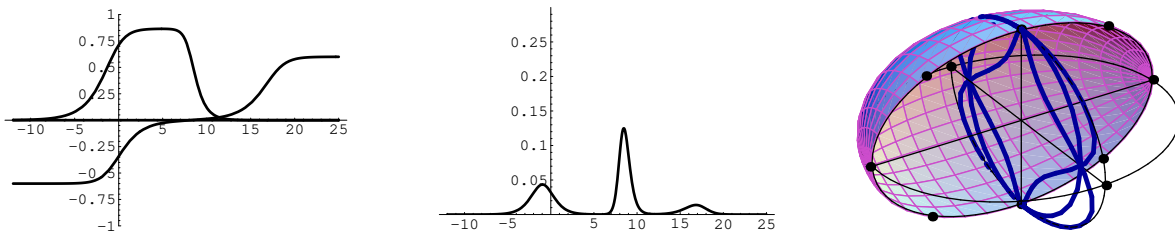


Figure 11: Kink form factor (a), energy density (b) and orbits (c) for K_4^{BB} kinks.

necessarily involves a force between them. Here, we are dealing with a static configuration of two pairs of

basic particles. Thus, a delicate balance between the $K_1^{OB}-K_1^{OB}$ and $K_1^{BC}-K_1^{BC}$ forces must be reached. This is only possible if one K_1^{OB} and one K_1^{BC} kink share exactly their centers in between the other two basic particles, see Figure 11(b). Any small perturbation of this situation would release forces, an argument for a dynamical explanation of instability. The fate of these solutions as time passes is explained in sub-Section 4.2 of Reference [14] for similar quadruple solitary waves arising in that model.

2. $K_4^{CC}(b)$: Another one-parametric family of kinks exists on the ellipsoid \mathbb{E} ($\lambda = 0$). The sign combinations $s_\mu \neq s_\nu$ in the system of equations (21) provide the solutions in the original fields:

$$\begin{aligned}\bar{\phi}_1(x) &= \frac{(-1)^\alpha \sigma_2 \sigma_3 (1 + e^{b e^{2\sqrt{2}\sigma_3^2 \bar{x}}})}{\sqrt{(\sigma_2^2 + \sigma_3^2 e^{b e^{2\sqrt{2}\sigma_3^2 \bar{x}}} + \sigma_3^2 e^{2\sqrt{2}\sigma_3^2 \bar{x}})(\sigma_3^2 + \sigma_2^2 e^{b e^{2\sqrt{2}\sigma_3^2 \bar{x}}} + \sigma_3^2 e^{b e^{-2\sqrt{2}\sigma_3^2 \bar{x}}})}} \\ \bar{\phi}_2(x) &= \frac{\sigma_2 \bar{\sigma}_2 \sigma_3 (1 + e^{-2\sqrt{2}\sigma_3^2 \bar{x}})}{\sqrt{(\sigma_3^2 + \sigma_2^2 e^{-2\sqrt{2}\sigma_3^2 \bar{x}} + \sigma_3^2 e^{b e^{-2\sqrt{2}\sigma_3^2 \bar{x}}})(\sigma_2^2 + \sigma_3^2 e^{-b e^{-2\sqrt{2}\sigma_3^2 \bar{x}}} + \sigma_3^2 e^{-2\sqrt{2}\sigma_3^2 \bar{x}})}} \\ \bar{\phi}_3(x) &= \frac{(-1)^\beta \sigma_3 \bar{\sigma}_3 \sigma_3 (1 + e^{b e^{-2\sqrt{2}\sigma_3^2 \bar{x}}})}{\sqrt{(\sigma_3^2 + \sigma_2^2 e^{-2\sqrt{2}\sigma_3^2 \bar{x}} + \sigma_3^2 e^{b e^{-2\sqrt{2}\sigma_3^2 \bar{x}}})(\sigma_3^2 + \sigma_2^2 e^{b e^{2\sqrt{2}\sigma_3^2 \bar{x}}} + \sigma_3^2 e^{b e^{-2\sqrt{2}\sigma_3^2 \bar{x}}})}}\end{aligned}$$

Two components are bell-shaped, ϕ_1 and ϕ_3 , whereas the third one, ϕ_2 , is of two-kink form, see Figure 12(a). $b = -\sqrt{2}\sigma_2^2\sigma_3^2\gamma_2$ is the parameter that characterizes the family members; the values $\alpha, \beta = 0, 1$ specify the quadrant of the ellipsoid \mathbb{E} in which the kink is located. These solitary waves belong to the C^{CC} topological sectors and connect the points C^+ and C^- crossing the umbilicus points A , see Figure 12(c). In Figure 12(a), a $K_4^{CC}(b)$ kink is depicted leaving from point C_- and arriving at C_+ as x goes from $-\infty$ to ∞ . In Figure 12(b) the energy density is shown, displayed by three lumps; two of them are easily identified as the basic particles K_1^{CD} and K_1^{BC} but the more energetic lump, located between the previous ones, corresponds to a combination forming the $K_2^{DB}(0)$ kink. Thus, the $K_4^{CC}(b)$ solutions are composites of four basic particles, two K_1^{CD} and two K_1^{BC} ones. The energy depends only the coupling constant σ_3 :

$$E[K_4^{CC}(b)] = E(K_1^{CB}) + E[K_2^{DB}(0)] + E(K_1^{DC}) = 2E(K_1^{CD}) + 2E(K_1^{BC}) = \frac{\sigma_3^2(2 - \sigma_3^2)}{\sqrt{2}}.$$

The $K_4^{CC}(b)$ four-body kinks are qualitatively identical to the $K_4^{BB}(b)$ kinks replacing the ellipsoid \mathbb{E}

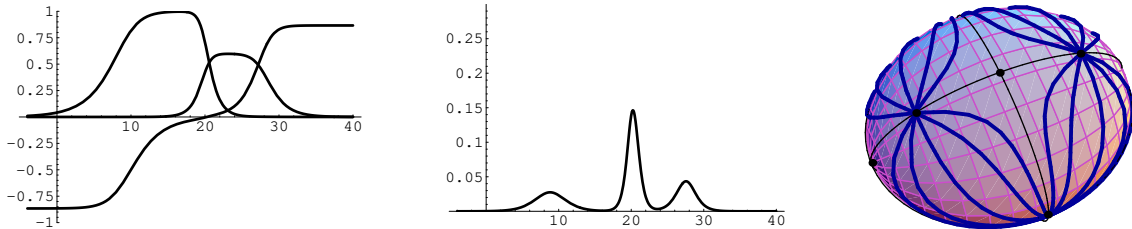


Figure 12: *Kink form factor (a), energy density (b) and orbits (c) for K_4^{CC} kinks.*

by the $\phi_1 = 0$ plane ($\lambda = 0$ and $\nu = 1$ faces in the $P(0)$ cuboid). Thus, all considerations about stability and forces made for the $K_4^{BB}(b)$ kinks also work for the $K_4^{CC}(b)$'s.

3.5 Six-body solitary waves

1. $K_6^{CC}(b)$: There is a more complicated one-parametric family of solitary waves in the C^{CC} topological sectors living in the $\phi_3 = 0$ plane. The potential is restricted

$$V(\phi_1, \phi_2, 0) = (\phi_1^2 + \phi_2^2)(\phi_1^2 + \phi_2^2 - 1)^2 + 2\sigma_2^2\phi_2^2(\phi_1^2 + \phi_2^2 - 1) + \sigma_2^4\phi_2^2$$

to that discussed in the two scalar field model of Reference [14]. In the present context, however, the Hamiltonian (14) reduces to either the I) $\lambda = \bar{\sigma}_3^2$ or II) $\mu = \bar{\sigma}_3^2$ faces of $P(0)$:

$$H_I = \frac{H_\mu}{(\mu - \bar{\sigma}_3^2)(\mu - \nu)} + \frac{H_\nu}{(\nu - \bar{\sigma}_3^2)(\nu - \mu)} \quad , \quad H_{II} = \frac{H_\lambda}{(\lambda - \bar{\sigma}_3^2)(\lambda - \nu)} + \frac{H_\nu}{(\nu - \lambda)(\nu - \bar{\sigma}_3^2)} \quad .$$

The Hamilton-Jacobi equations for H_I and H_{II} must be solved consecutively and the two pieces should be continuously glued afterwards, see Reference [23] for similar solutions in a simpler model with a quartic potential energy. Sign combinations for s_λ, s_μ, s_ν leading to these solitary waves are different from those giving the $K_3^{OD}(0, b)$ kinks.

These solutions connect the points C^+ and C^- and cross the F_2 foci (see Figure 12(c)). The kink form factors are:

$$\begin{aligned} \bar{\phi}_1(x) &= \frac{(-1)^\alpha \sigma_2 \left(1 + e^{2\sqrt{2}\bar{\sigma}_2^2 x}\right)}{\sqrt{\sigma_2^2 + \bar{\sigma}_2^2 e^{-b} e^{-2\sqrt{2}\bar{x}} + e^{2\sqrt{2}\bar{\sigma}_2^2 x} \sqrt{1 + \sigma_2^2 e^{2\sqrt{2}\bar{\sigma}_2^2 x} + \bar{\sigma}_2^2 e^b e^{-2\sqrt{2}\bar{\sigma}_2^2 x}}} \\ \bar{\phi}_2(x) &= \frac{\sigma_2 \bar{\sigma}_2^2 \left(e^{2\sqrt{2}\bar{x}} - e^b\right)}{\sqrt{e^{2\sqrt{2}\bar{\sigma}_2^2 x} + \sigma_2^2 e^{2\sqrt{2}\bar{x}} + \bar{\sigma}_2^2 e^b \sqrt{e^b e^{2\sqrt{2}\bar{\sigma}_2^2 x} + \sigma_2^2 e^b + \bar{\sigma}_2^2 e^{2\sqrt{2}\bar{x}}}} \\ \bar{\phi}_3(x) &= 0 \end{aligned} \quad .$$

In particular, a $K_6^{CC}(b)$ kink with $\alpha = 0$ has been depicted in Figure 12(a), departing from the point C_- and arriving in C_+ when x goes from $-\infty$ to ∞ . One component is of bell form and the other is two kink-shaped. In Figure 12(b) the $K_6^{CC}(b)$ energy density is shown. Apparently, these solutions are formed by three lumps. One of them is the basic particle K_1^{CD} ; the more energetic lump in the middle of the other two is the $K_3^{OD}(0)$ kink (the union of the three basic particles), and the third lump is a K_2^{OC} kink (superposition of the K_1^{OB} and K_1^{BC} basic kinks). Therefore, the $K_6^{CC}(b)$ solutions involve six basic particles, a pair of each type of basic lumps. These static configurations describe an even more delicate equilibrium than four-body lumps. The forces between basic kinks of the same type are only balanced at the expense of joining them in a arrangement such as that shown in Figure 12(b). Any relative displacement of the centers of the composite particles would destroy these unstable solutions. The energy of these six-body solitary waves does not depend on the coupling constants:

$$E[K_6^{CC}(b)] = E(K_1^{CD}) + E[K_3^{DO}(0, 0)] + E[K_2^{OC}(0)] = 2E(K_1^{CD}) + 2E(K_1^{OB}) + 2E(K_1^{BC}) = \frac{1}{\sqrt{2}} \quad .$$

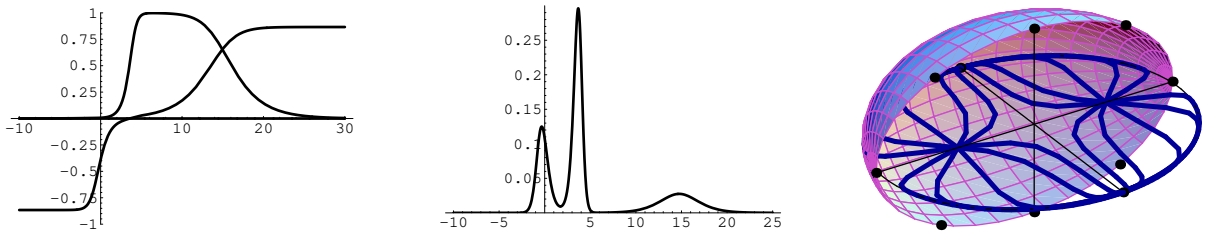


Figure 13: Kink form factor (a), energy density (b) and orbits (c) for K_6^{CC} kinks.

2. K_6^{BB} : Another one-parametric family of six-body solitary waves exists in the \mathcal{C}^{BB} topological sectors, now located on the plane $\phi_2 = 0$. Also, the restricted potential energy,

$$V(\phi_1, 0, \phi_2) = (\phi_1^2 + \phi_3^2)(\phi_1^2 + \phi_3^2 - 1)^2 + 2\sigma_3^2 \phi_3^2 (\phi_1^2 + \phi_2^2 + \phi_3^2 - 1) + \sigma_3^4 \phi_3^2 \quad ,$$

corresponds to a two-component scalar field model studied in [14]. There is one difference in this three-component situation: as in the previous case, the Hamiltonian (14) reduces to either the I) $\mu = \bar{\sigma}_2^2$ or II) $\nu = \bar{\sigma}_2^2$ faces of $P(0)$:

$$H_I = \frac{H_\lambda}{(\lambda - \bar{\sigma}_2^2)(\lambda - \nu)} + \frac{H_\nu}{(\nu - \lambda)(\nu - \bar{\sigma}_2^2)} \quad , \quad H_{II} = \frac{H_\lambda}{(\lambda - \mu)(\lambda - \bar{\sigma}_2^2)} + \frac{H_\mu}{(\mu - \lambda)(\mu - \bar{\sigma}_2^2)} \quad .$$

Again, the Hamilton-Jacobi equations for H_I and H_{II} must be solved consecutively and the two pieces must be continuously glued afterwards. The choice of sign combinations for s_λ, s_μ, s_ν is opposite to that giving the $K_3^{OD}(a, 0)$ kinks.

These solutions asymptotically join the points B^+ and B^- crossing the foci F_3 . The kink form factors are:

$$\begin{aligned} \bar{\phi}_1(x) &= \frac{(-1)^\alpha \sigma_3 \left(1 + e^{2\sqrt{2}\bar{\sigma}_3^2 x}\right)}{\sqrt{\sigma_3^2 + \bar{\sigma}_3^2 e^{-b} e^{2\sqrt{2}x} + e^{2\sqrt{2}\bar{\sigma}_3^2 x} \sqrt{1 + \sigma_3^2 e^{2\sqrt{2}\bar{\sigma}_3^2 x} + \bar{\sigma}_3^2 e^b e^{-2\sqrt{2}\bar{\sigma}_3^2 x}}}} \\ \bar{\phi}_2(x) &= 0 \\ \bar{\phi}_3(x) &= \frac{\sigma_3 \bar{\sigma}_3^2 \left(e^{2\sqrt{2}x} - e^b\right)}{\sqrt{e^{2\sqrt{2}\bar{\sigma}_3^2 x} + \sigma_3^2 e^{2\sqrt{2}x} + \bar{\sigma}_3^2 e^b \sqrt{e^b e^{2\sqrt{2}\bar{\sigma}_3^2 x} + \sigma_3^2 e^b + \bar{\sigma}_3^2 e^{2\sqrt{2}x}}}} \quad . \end{aligned}$$

In Figure 14(a) a K_6^{BB} kink is depicted with $\alpha = 0$ that connects the point B_- with B_+ . The structure of one member of this family is similar to that found for the previous kinks. From the energy density plot shown in Figure 14(b), one sees that each member of the family consists of six basic particles: two K_1^{CD} , two K_1^{OB} and two K_1^{BC} kinks. Only the order differs (the two-body kink is on the right of the three-body lump) and the two-body kink is made of a K_1^{CD} and a K_1^{BC} solitary wave, instead of a K_1^{OB} and a K_1^{BC} . The energy, however, is the same:

$$E(K_6^{BB}) = E(K_1^{BO}) + E(K_3^{OD}(0, 0)) + E(K_2^{DB}) = 2E(K_1^{CD}) + 2E(K_1^{OB}) + 2E(K_2^{BC}) = \frac{1}{\sqrt{2}} \quad .$$

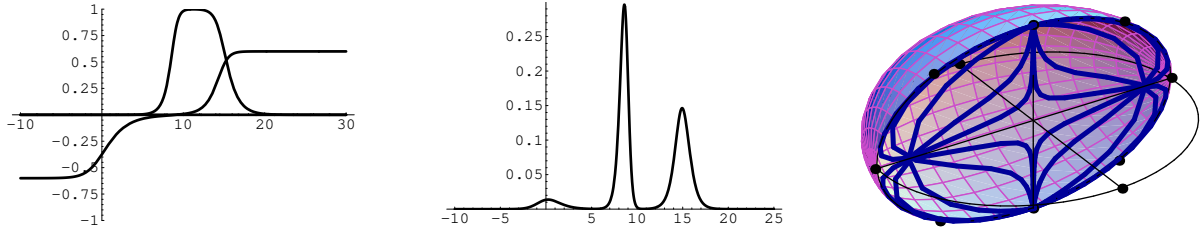


Figure 14: *Kink form factor (a), energy density (b) and orbits (c) for K_6^{BB} kinks.*

3.6 Seven-body solitary waves

2. $K_7^{BC}(\gamma_2, \gamma_3)$: Besides the generic (depending on two parameters) $K_3^{OD}(a, b)$ kinks, there are other generic solitary waves. Other combinations of signs in the system of equations (23) provide new generic kinks different from $K_3^{OD}(a, b)$. The kink orbits of these solutions run between the B and C minima tracing a curve with three well-defined stages: 1) First, the kink trajectory departs from the point C at $x = -\infty$ remaining in a octant of the ellipsoid \mathbb{E} interior until the particle reaches a point of the characteristic hyperbola h . During this stage the trajectory satisfies the system of equations (23) with

$s_\lambda = s_\mu \neq s_\nu$. 2) Then, the kink orbit crosses to the next octant (from left to right or viceversa) through this point and traces a curve that ends by hitting a point in the characteristic ellipse e_4 . In this second stage the kink trajectory also complies with (23) but the sign combination is $s_\lambda = s_\nu \neq s_\mu$. 3) The last stage of the kink trajectory starts again by changing the octant (from up to down or viceversa) through the point in e_4 . The kink orbit runs along a curve in the latter octant until the point B is reached. The final stage satisfies the system (23) with $s_\lambda \neq s_\mu = s_\nu$, see Figure 15(c). The parameters γ_2 and γ_3 respectively determine the points where the kink orbit hits the characteristic hyperbola h and ellipse e_4 . Orbits for which the relation $\gamma_2 - \bar{\sigma}_3^2 \gamma_3$ between integration constants holds meet at a single point on ellipse e_4 . The same happens for trajectories that comply with $\gamma_2 - \bar{\sigma}_2^2 \gamma_3$ meeting at a point on the hyperbola h . Thus, at each point in h and e_4 an infinite number of kink trajectories meet. These characteristic curves are focal lines.

These solutions are so complex that it is not possible to invert the relationships (23) in order to obtain analytical expressions in Cartesian coordinates for the kink form factors. For this reason, we parametrize these solutions in terms of the integration constants γ_2 and γ_3 that set the orbits in the Hamilton-Jacobi expressions (23). The use, however, of the implicit expressions in elliptic coordinates allows Mathematica to plot field profiles and energy densities. It should be mentioned that extreme care is necessary to guarantee continuity of the trajectories and its derivatives when it rebounds on the faces of the $P(0)$ cuboid. In Figure 15(a) the form factor (field profile) of a $K_7^{BC}(\gamma_2, \gamma_3)$ kink is shown. In the Figure 15(b) we display the energy showing seven basic lumps: two K_1^{CD} 's, two K_1^{OB} 's and three K_1^{BC} 's, with the peculiarity that three different basic particles always travel together. We remark that there exist no net forces between particles in these configurations but that they are highly unstable against any perturbation splitting the centers of superposed particles. The total energy is:

$$E(K_7^{BC}) = 2E(K_1^{CD}) + 2E(K_1^{OB}) + 3E(K_1^{BC}) = \frac{1}{\sqrt{2}} + \frac{\bar{\sigma}_2^4 - \bar{\sigma}_3^4}{2\sqrt{2}}$$

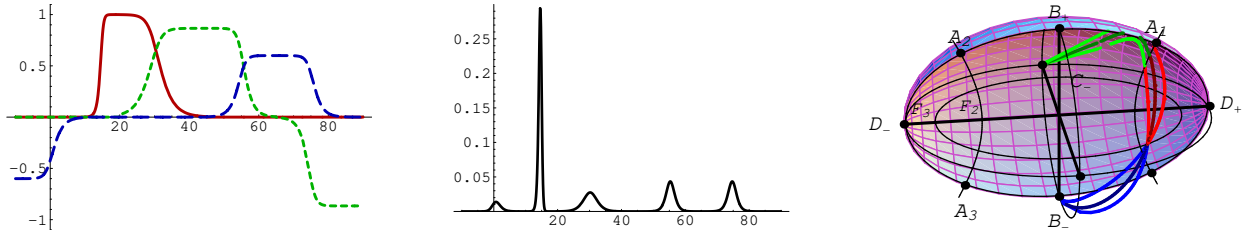


Figure 15: Kink form factor (a), energy density (b) and orbits (c) for K_7^{BC} kinks.

A summary of all the kink energies is offered in the following table:

Type of Kink	Energy		
Basic Kinks	$E(K_1^{OB}) = \frac{\bar{\sigma}_3^4}{2\sqrt{2}}$	$E(K_1^{CD}) = \frac{\sigma_2^2(2-\sigma_2^2)}{2\sqrt{2}}$	$E(K_1^{BC}) = \frac{\bar{\sigma}_2^4 - \bar{\sigma}_3^4}{2\sqrt{2}}$
Two-Body Kinks	$E[K_2^{OC}(b)] = \frac{\bar{\sigma}_2^4}{2\sqrt{2}}$	$E[K_2^{BD}(b)] = \frac{\sigma_3^2(2-\sigma_3^2)}{2\sqrt{2}}$	
Three-Body Kinks	$E[K_3^{OD}(a, b)] = \frac{1}{2\sqrt{2}}$		
Four-Body Kinks	$E[K_4^{BB}(b)] = \frac{\bar{\sigma}_2^4}{\sqrt{2}}$	$E[K_4^{CC}(b)] = \frac{\sigma_3^2(2-\sigma_3^2)}{\sqrt{2}}$	
Six-Body Kinks	$E[K_6^{CC}(b)] = \frac{1}{\sqrt{2}}$	$E[K_6^{BB}(b)] = \frac{1}{\sqrt{2}}$	
Seven-Body Kinks	$E[K_7^{BC}(a, b)] = \frac{1}{\sqrt{2}} + \frac{\bar{\sigma}_2^4 - \bar{\sigma}_3^4}{2\sqrt{2}}$		

References

- [1] P.G. Drazin, R.S. Johnson; *Solitons: an introduction.*, Cambridge University Press. 1989.
- [2] A.H. Eschenfelder, *Magnetic Bubble Technology*, (1981) Berlin, Springer-Verlag.
- [3] F. Jona and G. Shirane, *Ferroelectric Crystals*, (1993) New York, Dover; E.K. Salje, *Phase Transitions in Ferroelastic and Co-Elastic Crystals*, Cambridge, UK, Cambridge University Press; B.A. Strukov and A. Levanyuk, *Ferroelectric Phenomena in Crystals*, Berlin, Springer-Verlag.
- [4] F. Zhang and M. A. Collins *Topological solitons in polyethylene crystals*, Phys. Rev. E 49, 5804-5811 (1994); D. Bazeia and E. Ventura, *Topological twistons in crystalline polyethylene*, Chem. Phys. Lett., 303 (1999) 341-346; E. Ventura, A. M. Simas and D. Bazeia, *Exact topological twistons in crystalline polyethylene*, Chem. Phys. Lett., 320 (2000) 587-593; D. Bazeia, M.Z. Hernandez, A.M. Simas, *Solitons in Poly(oxyethylene)*, cond-mat/0207716.
- [5] J.M. Harris, *Poly(ethylene glycol) chemistry: Biotechnical and Biomedical Applications*, (1992) New York, Plenum.
- [6] A. Vilenkin and E.P.S. Shellard, *Cosmic Strings and Other Topological defects*, (1994) Cambridge, UK, Cambridge University Press.
- [7] S. Kobayashi, K. Koyama and J. Soda, Phys. Rev. **D65** (2002) 064014; C. Csaki, J. Erlich, T.J. Hollowood and Y. Shirman, Nucl. Phys. **B581** (2000) 309-338; M. Cvetič, Int. J. Mod. Phys. **A16** (2001) 891-899; O. DeWolfe, D.Z. Freedman, S.S. Gubser, A.Karch, Phys. Rev. **D62** (2000) 046008
- [8] H.M. Johng, H.S. Shin and K.S. Soh, Phys. Rev. **D53** (1996) 801; N.D. Antunes, E.J. Copeland, M. Hindmarsh and A. Lukas, *“Kinky brane worlds”*, Phys.Rev. D68 (2003) 066005
- [9] T. Banks and M. O’Loughlin, Nucl. Phys. **B449**, (1995); T. Damour and A. Vilenkin, Phys. Rev. **D53** (1996) 2981; A. Wang, Phys. Rev **D66** (2002) 024024
- [10] D. Olive and E. Witten, Phys. Lett. **B78** (1978) 97; N. Seiberg and E.Witten, Nucl. Phys. **B246** (1994) 19.
- [11] M. Duff, R. Khuri and J. Lu, Phys. Rep. **259** (1995) 213.
- [12] G. Dvali and M. Shifman, Nucl. Phys. **B504** (1997) 127; G. Gibbons and P. Townsend, Phys. Rev. Lett. **83** (1999) 172.
- [13] R. Rajaraman, *Solitons and instantons. An introduction to solitons and instantons in quantum field theory*, North-Holland Publishing Co. 1987.
- [14] A. Alonso Izquierdo, M.A. Gonzalez Leon, M. de la Torre Mayado, J. Mateos Guilarte, *“Changing shapes: adiabatic dynamics of composite solitary waves”*, Physica D **200** (2005) 220-241.
- [15] C. Montonen, *“On solitons with an Abelian charge in scalar field theories: (I) Classical theory and Bohr-Sommerfeld quantization”*, Nucl. Phys. B **112** (1976) 349-357.
- [16] H. Ito, *“Kink energy sum rule in a two-component scalar field model of 1+1 dimensions”*, Phys. Lett. A **112** (1985) 119-123.
- [17] D. Bazeia, M. J. Dos Santos and R. F. Ribeiro, *“Solitons in systems of coupled scalar fields”*, Phys. Lett. A **208** (1995) 84-88.

- [18] D. Bazeia, J. R. S. Nascimento, R. F. Ribeiro and D. Toledo, “*Soliton stability in systems of two real scalar fields*”, J. Phys. A **30** (1997) 8157-8166.
- [19] A. Alonso Izquierdo, M.A. Gonzalez Leon, J. Mateos Guilarte and M. de la Torre Mayado, “*Kink variety in systems of two coupled scalar fields in two space-time dimensions*”, Phys. Rev. D **65** (2002) 085012.
- [20] A. Alonso Izquierdo, M.A. Gonzalez Leon, J. Mateos Guilarte and M. de la Torre Mayado, “*Adiabatic motion of two-component BPS kinks*”, Phys. Rev. D **66** (2002) 105022.
- [21] A. Alonso Izquierdo, M. A. Gonzalez Leon, and J. Mateos Guilarte, “*Kink manifolds in (1+1)-dimensional scalar field theory*”, J. Phys. A: Math. Gen. **31** (1998), 209-229.
- [22] N. Manton, “*A remark on the scattering of BPS monopoles*”, Phys. Lett. B **110** (1982) 54-56.
- [23] A. Alonso Izquierdo, M. A. Gonzalez Leon, and J. Mateos Guilarte, “*Kink from dynamical systems: domain walls in a deformed $O(N)$ linear sigma model*”, Nonlinearity **13** (2000), 1137-1169.
- [24] A. Alonso Izquierdo, M. A. Gonzalez Leon, and J. Mateos Guilarte, “*Stability of kink defects in a deformed $O(3)$ linear sigma model*”, Nonlinearity **15** (2002), 1097-1125.
- [25] A. Alonso Izquierdo, J.C. Bueno Sánchez, M. A. Gonzalez Leon, and M. de la Torre Mayado, “*Kink manifolds in a three-component scalar field theory*”, J. Phys. A: Math. Gen. **37** (2004), 3607-3626.
- [26] D. Bazeia, L. Losano, C. Wotzasek, “*Domain walls in three-field models*”, Phys.Rev. **D66** (2002) 105025
- [27] D. Bazeia and F. A. Brito, *Entrapment of a network of domain walls* Phys. Rev. **D62** (2000) 101701.
- [28] P. Sutcliffe, *Domain wall networks on solitons*, Phys. Rev. **D68**, 085004 (2003).
- [29] D. Bazeia, H. Boschi-Filho, F.A. Brito, *Domain defects in systems of two real scalar fields* JHEP **028** (1999) 9904; J.D. Edelstein, M.L. Trobo, F.A. Brito, D. Bazeia, *Kinks Inside Supersymmetric Domain Ribbons*, Phys.Rev. **D57** (1998) 7561-7569.
- [30] J.R. Morris, *Nested Domain Defects* Int. J. Mod. Phys. **A13** (1998) 1115-1128.
- [31] D. Bazeia, F.A. Brito, L. Losano, *Relaxing to a three dimensional brane junction*, hep-th/0512331.
- [32] P.P. Avelino, C.J.A.P. Martins, J. Menezes, R. Menezes, J.C.R.E. Oliveira, *Defect Junctions and Domain Wall Dynamics*, hep-ph/0604250
- [33] S. Coleman, “*There are no Goldstone bosons in two dimensions*”, Com. Math. Phys. **31** (1973) 259-264.
- [34] H. Ito and H. Tasaki, “*Stability theory for nonlinear Klein-Gordon Kinks and Morse’s index theorem*”, Phys. Lett. A **113** (1985) 179-182.
- [35] J. Mateos Guilarte, *A note on Morse theory and one-dimensional solitons*, Lett. Math. Phys. **14** (1987) 169-176, “*Stationary phase approximation and quantum soliton families*”, Ann. Phys, **188** (1988) 307-346.